



**HAL**  
open science

# Evidence of elevation effect on stable isotopes of water along highlands of a humid tropical mountain belt (Western Ghats, India) experiencing monsoonal climate

M. Tripti, L. Lambs, I. Moussa, D. Corenblit

## ► To cite this version:

M. Tripti, L. Lambs, I. Moussa, D. Corenblit. Evidence of elevation effect on stable isotopes of water along highlands of a humid tropical mountain belt (Western Ghats, India) experiencing monsoonal climate. *Journal of Hydrology*, 2019, 573, pp.469-485. 10.1016/j.jhydrol.2019.03.086 . hal-02180290v2

**HAL Id: hal-02180290**

**<https://hal.science/hal-02180290v2>**

Submitted on 22 Oct 2021

**HAL** is a multi-disciplinary open access archive for the deposit and dissemination of scientific research documents, whether they are published or not. The documents may come from teaching and research institutions in France or abroad, or from public or private research centers.

L'archive ouverte pluridisciplinaire **HAL**, est destinée au dépôt et à la diffusion de documents scientifiques de niveau recherche, publiés ou non, émanant des établissements d'enseignement et de recherche français ou étrangers, des laboratoires publics ou privés.



Distributed under a Creative Commons Attribution - NonCommercial 4.0 International License

1 **Evidence of elevation effect on stable isotopes of water along highlands of a humid**  
2 **tropical mountain belt (Western Ghats, India) experiencing monsoonal climate**

3 **M. Tripti<sup>1,2</sup>, L. Lambs<sup>1,\*</sup>, I. Moussa<sup>1</sup>, D. Corenblit<sup>1,3</sup>**

4 <sup>1</sup>Ecolab, Université de Toulouse III, Paul Sabatier University, CNRS, INPT, 118 route de  
5 Narbonne, F-31062 Toulouse, France.

6 <sup>2</sup>National Centre for Earth Science Studies, Ministry of Earth Sciences, Akkulam, 695011  
7 Thiruvananthapuram, India.

8 <sup>3</sup>Université Clermont Auvergne, CNRS, GEOLAB, F-63000 Clermont-Ferrand, France.

9 \*Corresponding author: [luc.lambs@univ-tlse3.fr](mailto:luc.lambs@univ-tlse3.fr)

10

11 **Abstract**

12 Forest ecosystem plays a major role in controlling moisture dynamics over the continents,  
13 particularly in the humid tropics. The montane forest ecosystem in South India supports a  
14 characteristic warm tropical climate which affects the weather pattern and the monsoon  
15 system. This study focuses on better understanding of the influence of dual monsoonal rainfall  
16 on the surface water and groundwater in south-west India, and the role of the Western Ghats  
17 mountain belt in governing the water isotope characteristics (i.e., *isotopic elevation, rainfall*  
18 *amount and continental effects*) in the humid tropics of South India. This is achieved through  
19 a spatial study of stable isotope ratios of surface and subsurface water (oxygen,  $\delta^{18}\text{O}$  and  
20 hydrogen,  $\delta^2\text{H}$ ), collected from different tropical river basins located between Kozhikode  
21 (Kerala, 10° 30' N) and Udipi (Karnataka, 13° 30' N), in the wettest places and highest peaks  
22 of the Western Ghats between 2011 and 2014. The results on stable isotope ratios of ground

23 water and springs show that the water from the tropical mountain belt of the Western Ghats  
24 exhibit a low elevation effect with an isotopic lapse rate of 0.09 ‰/100 m for  $\delta^{18}\text{O}$  up to 2050  
25 m asl. Beyond 2050 m asl, a considerable effect of elevation with an isotopic lapse rate of 2.5  
26 ‰/100 m for  $\delta^{18}\text{O}$  is observed. The water samples from the Nilgiri ranges (1950-2300 m asl)  
27 exhibited higher isotopic lapse rate of 1.5 ‰/100 m for  $\delta^{18}\text{O}$  unlike that of the mountains  
28 (Ezhimala, Agumbe and Chembra) close to the eastern Arabian Sea. The difference in  
29 isotopic lapse rate is mainly dependent on (i) the dominating seasonality of oceanic source  
30 moisture over the subcontinent leading to higher depletion of heavy isotopes for more inland  
31 groundwater during the winter monsoon on the eastern slopes of the Western Ghats (ii) the  
32 degree of terrestrial moisture feedback mechanisms along the windward slopes of the Ghats  
33 belt (i.e., Arabian Sea coast of India) leading to relative enrichment of heavy isotopes in  
34 groundwater fed by the highly recycled vapour sources rather than depletion due to amount,  
35 elevation or continental effect, and iii) deep cooling of orographically uplifted air moisture at  
36 high elevations of inland tropical mountains. The observed isotopic elevation effect on the  
37 groundwater and surface water is unique and constrained by specific time scale and mountain  
38 ranges within the Western Ghats belt. This study provides new understanding on factors  
39 controlling hydrological budget along higher parts of the Western Ghats mountain belt in  
40 South India experiencing humid tropical climate.

#### 41 **Keywords**

42 Water cycle; stable isotope; isotopic elevation (altitude) effect; tropical mountainous river,  
43 spring, groundwater, Indian monsoon; Western Ghats

44

45

46

## 47 **1. Introduction**

48 The rich terrestrial biodiversity in the world is harboured by the humid tropical forests, which  
49 cover about 19.6 million km<sup>2</sup> of Earth's surface ([Pimm and Sugden, 1994](#)). Asia has the  
50 second largest humid tropical forest area, after South America with its huge Amazon basin.  
51 The humid tropical forests are localized over the hills and mountains in Asia, particularly in  
52 the Indian subcontinent, and play a crucial role in controlling the regional moisture dynamics.  
53 About half the world population lives in this part of Asia where agriculture (mainly rice and  
54 wheat) depends on the monsoon rainfall. The disequilibrium in heating system of water and  
55 land over the Earth's surface leads to change in moisture laden wind direction which in turn  
56 supports seasonality of monsoon rainfall. During the summer monsoon season (June -  
57 September), there is a large flow of air moisture from the ocean towards land and this flow is  
58 reversed during the winter monsoon season (October – December) leading to dual monsoon  
59 system in the subcontinent. The availability of continuous flow of moisture over the humid  
60 tropical regions makes it a prominent zone of anthropogenic activities. Although  
61 anthropogenic influence has been active in tropical regions for thousands of years, the  
62 encroachment over the humid forest ecosystem has been intense in recent decades. This rapid  
63 pace of change in the humid tropical forest directly impacted the global climate ([Vitousek et](#)  
64 [al., 1997](#)). However, the seasonal climatic variability over the tropics is caused by the  
65 monsoonal precipitation which is largely influenced by the Inter-Tropical Convergence Zone  
66 (ITCZ). As the ITCZs do not remain the same throughout the year, the tropical zones  
67 experience a wet summer monsoon and a dry winter monsoon as a part of the Hadley cycle.  
68 Consequently, the tropical regions exhibit less seasonal variability in stable isotope ratios  
69 (oxygen isotope ratio,  $\delta^{18}\text{O}$  and hydrogen isotope ratio,  $\delta^2\text{H}$ ) of precipitation with temperature  
70 compared to other climatic regions, as the precipitation is predominantly convective in nature  
71 ([Sturm et al., 2007](#)). In addition, the small seasonal temperature variability in the tropical

72 region results in lesser seasonal variability of  $\delta^{18}\text{O}$  and  $\delta^2\text{H}$  in precipitation (Clark and Fritz,  
73 1997). Thus, it is necessary to determine whether the variability in precipitation over the  
74 tropics is limited to the strong seasonality of monsoon moisture source, or strongly influenced  
75 by topography and the moisture feedback mechanisms over the continent.

76

### 77 1.1. Motivation

78 The impact of land-sea thermal contrast between Indian Ocean and Tibetan Plateau has been  
79 critical for the onset and variability of Asian Summer Monsoon (Li and Yanai, 1996). The  
80 major source of Indian Summer Monsoon (ISM) is the moisture brought by south-westerly  
81 winds from northern Indian Ocean and Arabian Sea leading to rain along the west coast of  
82 India and in the central and eastern parts of the Peninsula. The winter monsoon rain derives  
83 moisture carried by the north-easterly winds moving from the Bay of Bengal, South China  
84 Sea and continental vapour sources to provide precipitation to the eastern and south-eastern  
85 parts of the Peninsular India (Mooley and Shukla, 1987). These two sources of moisture in the  
86 two monsoon seasons are known to have distinct stable isotope ratios ( $\delta^{18}\text{O}$  and  $\delta^2\text{H}$ ) whose  
87 imprints are identifiable in the geographic distribution of isotopes in groundwater and surface  
88 water (Deshpande et al., 2003; Tripti et al. 2016) and rain water (Lekshmy et al 2014; Warriar  
89 et al., 2010).

90 A swift transition in monsoonal moisture distribution across short distances due to orography  
91 is also well documented in the south Asian region (Biasutti et al., 2012; Xie et al., 2006). In  
92 India, the two mountain ranges, i.e. the Himalayas (5000 - 8000 m asl) in the north and the  
93 Western Ghats (700 - 2500 m asl) in the south, act as critical barriers for the moisture laden  
94 winds leading to non-uniform monsoon rains over the subcontinent. In general, the  
95 orographically induced monsoon regions experience heavy rainfall on the windward side

96 whereas a higher aridity is observed on the leeward side of the mountain ranges (Day et al.,  
97 2015). This non-uniform distribution of moisture over the continent is evident from the  
98 distinct signatures of stable isotope ratios of rain water monitored for a particular location,  
99 plateau and individual river basin in South India (Rahul et al., 2016; Resmi et al., 2016;  
100 Yadava et al 2007). The  $\delta^2\text{H}$  data compiled for the precipitation and surface water over the  
101 Indian subcontinent shows homogenous signature in southern part with relatively higher  
102 isotope ratio ( $\delta^2\text{H} > -20 \text{‰}$ ) than the north and northeast India due to larger influence of  
103 southwest monsoon (Hobson et al., 2012). The initial analysis on impact of climatic  
104 conditions on water budgeting and local moisture recycling in the central part of the Western  
105 Ghats through stable isotopes of rainwater, river water and groundwater have been reported in  
106 our earlier study (Tripti et al., 2016). This study is carried out to provide a spatial monitoring  
107 of water isotopes on a synoptic scale of the Western Ghats to account for the hydrological  
108 budgeting and monsoonal climate along the humid tropical high mountains.

109

## 110 1.2. Historical background and current status of knowledge

111 To understand the hydrological cycle and its controlling secondary processes in large  
112 ecologically sensitive and critical geomorphic area, there is a need to apply adapted tools and  
113 models (McDonnell and Beven, 2014). Stable isotope hydrology is based on interpretation of  
114 isotope ratio ( $\delta^2\text{H}$ ,  $\delta^{18}\text{O}$ ) and its secondary parameter (deuterium-excess,  $d = \delta^2\text{H} - 8 \times \delta^{18}\text{O}$ ;  
115 Dansgaard, 1964) variability in precipitation which are governed by the origin of moisture  
116 and cloud processes (Kaseke et al., 2018; Stumpp et al., 2014). Following the pioneering  
117 stable isotope works in 1960s (Craig, 1961; Dansgaard, 1964; Epstein and Mayeda, 1953),  
118 there has been a significant improvement in our understanding of hydrological cycle on a  
119 global scale. Several studies have reported the main factors controlling composition of natural

120 isotopes in precipitation, and established their huge potential for the identification of water  
121 origin and characterization of hydrological systems (Froehlich et al., 1998; Vitvar et al.,  
122 2004). Stable isotopes were used to address watershed scale analysis only later in 1970s.  
123 Stable isotope tracers have proven to be useful in addressing basic water-focused questions  
124 such as origin, flow path, mixing and residence time in the watershed (Dincer et al., 1970;  
125 Kendall and McDonnell, 1998; Sklash, 1990). These questions form the basis for  
126 understanding water availability, biogeochemical cycling, microbial production and other  
127 ecological processes (McGuire and McDonnell, 2007).

128 It has been well documented that the distribution of precipitation isotopes depends on the  
129 local temperature, latitude and elevation (Dansgaard, 1964; Friedman et al., 1964). For  
130 instance, in the temperate regions, isotopic variations in precipitation have been correlated  
131 with mean surface air temperatures (Aggarwal et al., 2012; Araguas-Araguas et al., 2000;  
132 Bowen, 2008; Dansgaard, 1964; Rozanski et al., 1993; Sanchez-Murillo et al., 2013) whereas  
133 in the tropics, several studies have reported the *rainfall amount effect* as the main controlling  
134 factor (Bowen and Revenaugh, 2003; Rozanski et al., 1993). These controlling parameters  
135 create an observable spatial and temporal variability in isotopic composition of water over a  
136 geographic region which is large enough to trace regional and global patterns (Bowen et al.,  
137 2009).

138 Further, few studies on the mountainous tropical regions (Lachniet and Patterson, 2002, 2009;  
139 Vuille et al., 2003) highlight the need for long-term monitoring networks to trace the impact  
140 of orographic effect, moisture recycling and canopy interception, intense evapotranspiration,  
141 and microclimate on the variability of isotopic composition of water. This study on the  
142 Western Ghats, India aims to bring a better understanding on this tropical mountain belt  
143 influencing the monsoonal rainfall characteristics through stable isotope investigation of  
144 surface and sub-surface water over a period of four years observation (2011-2014). In

145 particular, this work deals with three major factors: (i) the *elevation effect*, (ii) the *rainfall*  
146 *amount effect* and (iii) the *continental effect*. This is discussed in detail below.

147 (i) The *elevation effect*: Stable isotopes of water have been a useful proxy for understanding  
148 the paleo-elevation changes of the mountains from different geographical regions  
149 (Chamberlain and Poage, 2000). Moreover, the stable isotopes of water are conservative in  
150 their mixing relationship and for explaining flow paths (McGuire and McDonnell, 2007). It is  
151 well documented that water at higher elevation is highly depleted in heavy isotopes ( $^{18}\text{O}$  and  
152  $^2\text{H}$ ) because of Rayleigh distillation and orography (Poage and Chamberlain, 2001) although  
153 there are several secondary processes such as evaporation and isotope exchange with ambient  
154 vapour which can modify these isotopic signatures (Dansgaard, 1964; Siegenthaler and  
155 Oeschger, 1980). In general, the orographically uplifted cooler air mass condenses to form  
156 vapour and precipitation which are lighter ( $^{16}\text{O}$  and  $^1\text{H}$ ) in their isotopic composition relative  
157 to the original oceanic moisture brought by advection. Consequently, there is a relatively  
158 higher input of lighter isotopes (resulting in low  $\delta^{18}\text{O}$ ) to groundwater and surface water at  
159 high elevations and/or on the leeward side of mountain ranges than on the lower elevations of  
160 the windward side (Gonfiantini et al., 2001).

161 (ii) The *rainfall amount effect*: In addition to the *elevation effect*, there is a substantial  
162 temporal and spatial variability in the stable isotope ratios of precipitation in different  
163 ecosystems due to the rainfall amount effect (Dansgaard, 1964; Garcia et al., 1998; Gat, 1996;  
164 Gonfiantini et al., 2001; Rozanski et al., 1992; Siegenthaler and Oeschger, 1980; Windhorst et  
165 al., 2013). These studies have reported that the precipitation of higher amount exhibits lower  
166 stable isotope ratio due to enrichment of lighter isotopes whereas the lower precipitation  
167 amount exhibits higher stable isotope ratio due to enrichment of heavy isotopes. However,  
168 this difference in the stable isotope ratios with precipitation amount tends to be smaller in the  
169 tropical ecosystems (Scholl et al., 2009; Tripti et al., 2016) although there is a large variability



170 in precipitation amount. There are also studies reporting the reversed *rainfall amount effect* on  
171 the stable isotope ratios (i.e., a positive correlation of  $\delta^{18}\text{O}$  and  $\delta^2\text{H}$  with precipitation amount)  
172 of precipitation in the tropical region (Yadava et al., 2007).

173 (iii) The *continental effect*: This effect explains how the rainout system affects the isotopic  
174 composition of the rainfall and groundwater. The mean  $\delta^{18}\text{O}$  of groundwater in both across  
175 and along the region between eastern Arabian Sea coast and the western slopes of the Western  
176 Ghats is around  $-3 \pm 0.5$  ‰, and depicts the signature of homogeneous summer monsoon  
177 moisture input rather than that from the rainout history (Deshpande et al., 2003; Tripti et al.,  
178 2016). Recently the rain out effect has been reported for the west draining river basins of the  
179 Western Ghats where it is observed that the effect is limited only to the onset of summer  
180 monsoon and before the availability of excess moisture for undergoing recycling process  
181 (Tripti et al., 2018). Several studies (Deshpande et al., 2003, Kumar et al., 1982; Negrel et al.  
182 2011) have reported that more inland in the Deccan plateau, the contribution of the north-east  
183 monsoon is significant and the mean groundwater exhibits higher depletion of heavy isotopes  
184 with  $\delta^{18}\text{O}$  varying from -4 to -6 ‰. However, in the tropical semi-arid climatic region,  
185 evaporation and post-evaporation processes have a greater impact on water isotopes. Most of  
186 the streams are ephemeral and evapotranspiration exceeds rainfall. Farmers rely on  
187 groundwater for agriculture which leads to over-pumping problems and water table decline in  
188 this region of South India.

189 The identification of potential influence of these three effects on stable isotope ratio of water  
190 is crucial for a better understanding of hydrological budgeting, microclimate conditions and  
191 the past climatic changes as observed from paleo-records preserved in natural archives like  
192 paleowater, tree ring, speleothem, paleosol, etc.

193

194 1.3. Objectives of this study

195 The present study focuses on determining the *elevation effect* on the isotopic composition of  
196 surface and sub-surface water along the Western Ghats and its adjacent plateau in South India.  
197 The aim is to account for the major factors controlling the surface and sub-surface hydrology  
198 along the higher parts of mountain belt experiencing tropical monsoonal climate using stable  
199 water isotopes as a tracer. The study involves investigation of stable isotopic composition of  
200 groundwater from the Arabian Sea coast and contrasting hydrologic and climatic regions  
201 towards inland, between latitude 10° 30' N and 13° 30' N, i.e. from Thrissur (Kerala) to  
202 Agumbe (Karnataka). Whenever there was no well to access groundwater, water samples  
203 were taken from spring/rivulet and pond/lake.

204 The three objectives of this study were to evaluate the following effects:

205 (i) The *elevation effect* on the stable isotope ratio of surface and sub-surface water in the  
206 humid tropical mountain belt. Water samples were collected from higher peaks of the Western  
207 Ghats in Kudremukh (1100 m asl), Charmadi Ghats (1800 m asl), Mullayanagiri peak (1930  
208 m asl) and the Doddabetta peak in the Nilgiri range (2600 m asl), and compared with samples  
209 from lower elevations.

210 (ii) The *rainfall amount effect* along the tropical monsoon forest belt where there are  
211 discernible differences in the rainfall amount. The surface and sub-surface water from wetter  
212 inland places of the Western Ghats, such as Agumbe (Karnataka) and the Wayanad plateau  
213 around Sultan Bathery (Kerala) were sampled, and compared with those of coastal stations,  
214 such as Bakrabail and Kozhikode (Kerala).

215 (iii) The effect of terrestrial factors (*continental effect*) on the stable isotope ratios of water in  
216 the humid tropical mountain ecosystem. Water samples were collected from different hills of  
217 the Western Ghats that are very close to the Arabian Sea (within 5 km) at Ezhimala (200 m

218 asl) up to the peaks inland within a distance of about 110 km from the sea at Doddabetta  
219 (2600 m asl).

220 These objectives primarily provide the structural sub-headings used in the following sections  
221 of Materials and Methods, Results and Discussion.

222

## 223 **2. Study area and sampling sites**

### 224 *2.1. Study area*

225 The Western Ghats (or the Sahyadri range) are often referred as the water tower of South  
226 Indian rivers as they form the headwaters of several major and small (in terms of length)  
227 rivers in South India ([Ramachandra et al., 2016](#)). The Western Ghats mountain belt stretches  
228 in parallel to the eastern Arabian Sea coast for about 1600 km covering an area of around  
229 140,000 km<sup>2</sup> which is interrupted only by the 30 km Palghat Gap at around 11 °N latitude in  
230 Kerala, South India. This mountain belt hosts a globally significant geomorphic feature with  
231 its unique influence on the wide-scale biophysical and ecological processes over the Indian  
232 Peninsula ([UNESCO, 2012](#)). The Western Ghats provide orography required for the summer  
233 monsoon winds in its western part and acts as a climate barrier ([Gunnell, 1998; Tawde and](#)  
234 [Singh., 2015](#)) which makes the plateau arid in the eastern part due to rain shadow effect. The  
235 monsoon current strikes the west coast of Peninsula from west and south-west, meets the  
236 Western Ghats which presents an almost uninterrupted barrier ranging from 610 to 2134 m  
237 asl. The air mass moving across the Western Ghats deposits most of its moisture on the  
238 windward side of the mountain ranges, and then sweeps across the leeward side and interior  
239 of the Peninsula in the east. The orographic rainfall system leads to variability in the amount  
240 of precipitation along the mountain ranges of the Western Ghats. The higher monsoon  
241 moisture deposited over the Ghats crest results in the origin of several rivers at higher

242 elevations and the formation of different upper watersheds on either side of the Ghats slopes  
243 ([Jain et al., 2007](#)). On the western part of the Western Ghats scarp, several indentations have  
244 been created by a large number of short, perennial, torrential west flowing rivers (e.g.,  
245 Nethravati, Gurupur, Swarna, Chaliyar, Periyar, Sharavati, Kali, etc) which traverse the  
246 narrow coastal plains before discharging into the Arabian Sea through narrow outlets, creeks  
247 and estuaries (see Figure 1.a.).

248 Most of the larger South Indian Rivers (e.g., Godavari, Krishna and Kaveri) which flow in the  
249 east towards the Bay of Bengal have their origin in the Western Ghats. The Krishna River  
250 which is the fourth largest river in terms of basin area in India originates in the middle of the  
251 Western Ghats, near Mahabaleshwar at an elevation of about 1300 m asl. The southern basins  
252 are formed by its major tributaries, Tunga and Bhadra Rivers which originate at elevations  
253 ~1100 m asl on the leeward side of Kudremukh peak in Karnataka (see Figure 1.a.). Further  
254 south, the Kaveri (Cauvery) River originates at Talakaveri on the Brahmagiri Hills of the  
255 Kodagu district at an elevation of 1341 m asl. The river flows in a south-eastern direction for  
256 about 800 km through states like Karnataka, Kerala and Tamil Nadu, and descending the  
257 Eastern Ghats in a series of great falls ([Achyuthan et al., 2010](#)). It also hosts tributaries from  
258 the Nilgiris (Bhavani) and Annamalai (Amaravati), the two highest peaks (~ 2600 m asl) in  
259 South India. These river basins host larger tropical forest ecosystems.

260 The river basins of South India receive their maximum rainfall during the south-west  
261 monsoon. However, the depressions in the Bay of Bengal causing widespread heavy rains and  
262 cyclones contribute moisture to the river basins in the eastern part of the Western Ghats  
263 during the winter monsoon period. The rainfall map of South India is given in Figure 1.b.,  
264 where the asymmetry induced by the Western Ghats is well represented. On the windward  
265 side, the narrow Arabian Sea coast of India exhibit annual monsoon rainfall from 2500 to  
266 4000 mm with mostly a unimodal type (dominant summer monsoon). On the leeward side, the

267 monsoon is of bimodal type (dual monsoon system representing summer and winter  
268 monsoons) with annual rainfall dropping rapidly from 2500 to 500 mm. The regional monthly  
269 rainfall (India Meteorological Department, Government of India) of the sampling locations during  
270 2013 - 2014 is given in Figure 1.c. and the sampling month is marked by blue rectangle,  
271 between October and December representing the period after the summer monsoon. The  
272 annual rainfall amount and oxygen isotope ratio for selected locations is given in Figure 1.d.

273

## 274 *2.2. Sampling sites*

275 Earlier works ([Gurumurthy et al., 2015](#); [Lambs et al., 2011](#); [Tripti et al., 2013, 2016, 2018](#))  
276 involved groundwater and river water sampling from southern Karnataka on the Arabian Sea  
277 coast within the river basins of Swarna and Nethravati and the nearby Ghats (Kudremukh and  
278 Charmadi Ghats). For the purpose of this study, we sampled mainly groundwater, springs and  
279 pond water at higher elevations on the Arabian Sea coastal side of the Western Ghats, and  
280 also groundwater and lake water at the sources of east flowing rivers with their watersheds  
281 draining the eastern part of the Western Ghats.

282 <Please insert here Figure 1.a.>

283 <Please insert here Figure 1.b.>

284 <Please insert here Figure 1.c.>

285 <Please insert here Figure 1.d.>

286 < Please insert here Table 1>

287 Field sites have been selected for collecting representative samples to address the three major  
288 factors like elevation, rainfall amount and continental effects as described in the following  
289 sections.

#### 290 *2.2.1. Elevation effect*

291 To test the elevation effect, we have sampled water from isolated peaks exhibiting elevation  
292 greater than 2000 m asl from the Nilgiri ranges (covers 2500 km<sup>2</sup> area and hosts 24 peaks)  
293 which include Doddabetta peak (2640 m asl) and Mukurthi peak (2550 m asl). The elevations  
294 of these isolated peaks are higher than the average typical mountain hills (600 to 1300 m asl)  
295 of the Western Ghats. Before stating of minimal isotopic *elevation effect* in the Western  
296 Ghats, there was a need for spatial sampling at the level of the highest mountain belt of the  
297 Nilgiris.

#### 298 *2.2.2. Rainfall amount effect*

299 Outside the rain shadow effects of eastern side of the Western Ghats, there is strong rainfall  
300 amount variability along the west coast and at higher peaks in South India (Figures 1b and  
301 1c). The mean annual rainfall increases from South to North, i.e., Thrissur (latitude 10° 30' N;  
302 annual rainfall = 3000 mm) to Udupi (latitude 13° 30' N; annual rainfall = 4500 mm) which is  
303 nearly the maximum for a coastal station ([Gunnel, 1998](#)).

304 To test the rainfall effect, we sampled two wettest places of the Western Ghats, in Karnataka  
305 at Agumbe with rainfall traversing through Udupi with a mean value of 5500 mm, and in  
306 Kerala, i.e., the Wayanad plateau at Vythiri with rainfall traversing through Kozhikode with a  
307 mean value of 3800 mm. These stations display similar geographic features: relatively lower  
308 elevation (600 - 800 m asl), close to the Arabian Sea (40-45 km) and surrounded by higher  
309 peaks to intercept the monsoon rainfall with an increase of 500-1000 mm/year relative to the  
310 corresponding coastal station.

### 311 2.2.3. *Continental effect*

312 To test the distance from the sea/coastline and possible *continental effect*, sampling was  
313 performed in a midland station of north Kerala at Bakrabail and in the inland mountains like  
314 Agumbe and Nilgiris during November 2013 which are located at different distances from the  
315 Arabian Sea (refer Table 1). Additional sampling was undertaken during October 2014 from  
316 locations adjacent to coast at Ezhimala hill (12°01'N, 75°12'E) and Thottada (11° 50' N, 75°  
317 24'E) to obtain the signatures of the direct sea moisture. This area of North Kerala is unique  
318 as it is the single place of abrupt rocky spur (286 m asl), facing directly the Arabian Sea,  
319 along the long sandy coast in southwest India which was sampled for this study.

320

## 321 **3. Materials and Methods**

322 The methodology followed to investigate the three research questions, i.e. isotopic *elevation*  
323 *effect*, *rainfall amount effect* and *continental effect*, in view to understand the hydrological  
324 cycle in the study area (geographic stretch from Agumbe to Ooty) include sampling of the  
325 available groundwater, spring and lake on a wider scale of elevation, dry and wet areas, and  
326 their distance from the Arabian Sea (here after referred as 'distance to coastline/sea'). In this  
327 study, water sampling has been performed with the same hydrological condition under  
328 average water level condition during the end of the monsoon, from October to December  
329 depending on the location (Figure 1.c.). The main criteria of the sampled water were its  
330 isotopic composition ( $\delta^{18}\text{O}$  and  $\delta^2\text{H}$  values), and water conductivity and temperature,  
331 whenever available.

332

### 333 3.1. *Sampling and analysis of water for Stable isotopes*

334 About 50 water samples were collected during the winter monsoon season, soon after the  
335 withdrawal of summer monsoon, in November 2013 and October 2014 (Figure 1.c.). For the  
336 study of the *elevation effect*, thirteen water samples (groundwater, rivulet, spring and lake)  
337 were collected during November 2013 in the area of Mukurthi peak (Pykara lake) and  
338 Doddabetta peak between 1990 m to 2630 m asl. For the study of the *rainfall amount effect*,  
339 six water samples (groundwater, rivulet and pond) were collected in the area of Agumbe  
340 during November 2013 and seven (groundwater, rivulet and spring) in the area of the  
341 Wayanad plateau during October 2014. In addition, water samples (rivulet, ponds and pipe  
342 flow water from soil sub-surface layer) were collected during November 2013 in the area of  
343 Bakrabail (n = 5) and during October 2014 in the area of Ezhimala (n = 16) for the study of  
344 the *continental effect*.

345 The groundwater samples were collected from dug wells (or open well: OW) and hand pumps  
346 (or bore well: BW). Dug wells and hand pumps that are regularly used were chosen for  
347 sampling. In case of dug well sampling, the samples were collected by lifting the water using  
348 a polythene bucket. When dug well or hand pump were not available, water samples were  
349 taken from spring or rivulet and pond or lake, at a depth of 50 cm to avoid any surface  
350 evaporation effect. For each location, water samples in 10 ml glass vials with tight caps were  
351 collected for isotopic measurements. Water temperature ( $^{\circ}\text{C}$ , only in 2013) and electrical  
352 conductivity ( $\mu\text{S cm}^{-1}$ ) were determined on-site using HACH multi-parameter probes. The  
353 exact positions of the sample sites were located with a GPS. All the sampling sites are shown  
354 in Figure 1.a. and details are given in Table 1.

355 The samples were kept under room temperature until analysis of their stable isotope ratios  
356 ( $\delta^{18}\text{O}$  and  $\delta^2\text{H}$ ) on an Isoprime 100 continuous flow isotope ratio mass spectrometer  
357 (Isoprime, Cheadle Hulme, UK) coupled with a Geo-Multiflow for water–gas equilibration



358 (Elementar, Hanau, Germany). The stable isotope ratios of oxygen and hydrogen are defined  
359 with  $\delta$  notation and ‰ unit as suggested by [Craig \(1961\)](#) and redefined by [Coplen \(2011\)](#).

360 The  $\delta^{18}\text{O}$  value of oxygen isotope is defined as:

$$361 \quad \delta^{18}\text{O}_{\text{VSMOW-SLAP}} = \left( \left( \frac{{}^{18}\text{O}/{}^{16}\text{O}}{\text{sample}} / \left( \frac{{}^{18}\text{O}/{}^{16}\text{O}}{\text{standard}} \right) - 1 \right) \text{‰}$$

362 For hydrogen isotope, the  $\delta^2\text{H}$  value is defined as:

$$363 \quad \delta^2\text{H}_{\text{VSMOW-SLAP}} = \left( \left( \frac{{}^2\text{H}/{}^1\text{H}}{\text{sample}} / \left( \frac{{}^2\text{H}/{}^1\text{H}}{\text{standard}} \right) - 1 \right) \text{‰}$$

364 In the laboratory, 0.3 mL aliquot of water was transferred into capped 3.7 mL vial for  
365 analysis. The sample vials used for  $\delta^{18}\text{O}$  measurements were flushed offline with a gas  
366 mixture of 5%  $\text{CO}_2$  in helium. The operating vials were then left to equilibrate at  $40^\circ\text{C}$  for  
367 about 8 hr. The analytical precision of the measurements was  $\sim 0.2$  ‰. In order to measure  
368 the  $\delta^2\text{H}$  signatures of the samples, Hokko beads were added to the 3.7 mL vials containing  
369 water samples and internal standards, before the vials were flushed offline with a gas mixture  
370 of 5%  $\text{H}_2$  in helium. The operating vials were then left to equilibrate at  $40^\circ\text{C}$  for about 8 hr.  
371 The measurements were made in duplicate, and the typical reproducibility was  $\sim 2.0$  ‰. Four  
372 internal standards were used, namely:

$$373 \quad \text{W1 } (\delta^{18}\text{O} = -1.5 \pm 0.21 \text{ ‰}, \delta^2\text{H} = -5.0 \pm 2.1 \text{ ‰}),$$

$$374 \quad \text{W2 } (\delta^{18}\text{O} = -6.2 \pm 0.23 \text{ ‰}, \delta^2\text{H} = -38.0 \pm 2.4 \text{ ‰}),$$

$$375 \quad \text{W3 } (\delta^{18}\text{O} = -10.5 \pm 0.25 \text{ ‰}, \delta^2\text{H} = -68.0 \pm 1.7 \text{ ‰}),$$

$$376 \quad \text{W4 } (\delta^{18}\text{O} = -15.5 \pm 0.24 \text{ ‰}, \delta^2\text{H} = -110.0 \pm 2.7 \text{ ‰}),$$

377 They were regularly checked against international reference standards, V-SMOW and V-  
378 SLAP provided by the International Atomic Energy Agency (IAEA, Vienna).

379 The deuterium excess (d-excess) was calculated according to Craig's formula ([Craig, 1961](#)) as  
380 explained by [Dansgaard \(1964\)](#), i.e., d-excess (‰) =  $\delta^2\text{H} - 8 \times \delta^{18}\text{O}$ .

381

### 382 3.2. Air masses trajectory analysis

383 In order to better understand the hydrological conditions during sampling and origin of the  
384 previous rainfall, an air mass back trajectory model was used. The program for '*Hybrid Single*  
385 *Particle Lagrangian Integrated Trajectory Model*' (HYSPLIT) developed by National  
386 Oceanic and Atmospheric Administration (NOAA) has been run for the sampling dates of  
387 main stations. This model is run for the air masses back trajectories upto five days to check if  
388 any short term severe cyclonic event (generally the case during the winter monsoon over  
389 Indian subcontinent) has impacted the hydrological systems in the Western Ghats prior to  
390 sampling.

391

### 392 3.3. Statistical analysis

393 The simple mean, standard deviation and regression were calculated using Microsoft Excel  
394 2016, whereas the multiple linear regression analysis was performed using Past v. 3.15. The  
395 dependent variable was the  $\delta^{18}\text{O}$  values, and the independent variables were the elevation  
396 (elevation effect), the distance to coastline (*continental effect*) and the annual rainfall amount  
397 (*rainfall amount effect*).

398

## 399 4. Results

400 The physico-chemical parameters (temperature and electrical conductivity) and stable isotopic  
401 composition of water samples collected in hills and plateaus along the Western Ghats stretch  
402 are given in Table 2. The temperature of water measured onsite is reported here to understand  
403 its influence on the stable isotope ratios. It is observed that the water samples display lower  
404 oxygen isotope ratios, i.e., more negative  $\delta^{18}\text{O}$  values at low temperature regions (Figure

405 2.a.). The relationship of measured  $\delta^{18}\text{O}$  with water temperature for the study period exhibits  
406 a similar trend as observed for the global water ( $d\delta^{18}\text{O}/dT = 0.66 \text{‰}/^\circ\text{C}$ ; Dansgaard, 1964) but  
407 with a lower slope ( $d\delta^{18}\text{O}/dT = 0.36 \text{‰}/^\circ\text{C}$ ) as the monitored water samples correspond to  
408 higher temperature range (10-30  $^\circ\text{C}$ ). The electrical conductivity is also provided as it forms a  
409 proxy to predict the geologic bedrock composition and the water residence time. Most of the  
410 sampled groundwater and spring water (except in the bore well, BW and lake) display low  
411 ionic content, with a mean conductivity of  $39 \pm 20 \text{ }\mu\text{S}/\text{cm}$  ( $n = 33$ ) and close to that of  
412 rainwater ( $\sim 20 \text{ }\mu\text{S}/\text{cm}$ ). This is due to the presence of the dominant silicate rock in the basin  
413 and the abundant tropical monsoon rainfall which further leads to dilution. The highest  
414 conductivity values are measured in lakes where the water is stored for a longer time, and in  
415 bore well compared to open well with a mean value of  $229 \pm 126 \text{ }\mu\text{S}/\text{cm}$  ( $n = 11$ ). Human  
416 activity also leads to an increased conductivity as observed for the open well in the middle of  
417 the town of Sultan Bathery ( $231 \text{ }\mu\text{S}/\text{cm}$ ) and for the Ooty Lake ( $450 \text{ }\mu\text{S}/\text{cm}$ ). The high values  
418 for the coastal sampling of the river and rivulet at Thottada (up to  $387 \text{ }\mu\text{S}/\text{cm}$ ) arise certainly  
419 from moderate saline intrusion. Thus, the conductivity of sampled water in these tropical  
420 mountainous regions varies between  $20 \text{ }\mu\text{S}/\text{cm}$  and  $500 \text{ }\mu\text{S}/\text{cm}$  depicting higher rainwater  
421 input to more water-rock interaction and anthropogenic interventions respectively. The  
422 relationship between conductivity and  $\delta^{18}\text{O}$  values is shown in Figure 2.b.

423 <please insert here Fig 2.a.>

424 <please insert here Fig 2.b.>

425 The overall relationship of  $\delta^{18}\text{O}$  versus  $\delta^2\text{H}$  is shown in Figure 3. Most of the samples fall on  
426 the Global Meteoric Water Line (GMWL) as defined by Craig (1961). Few samples of pond  
427 and lake are located below the GMWL with deuterium excess (d-excess) values ranging from  
428  $-2.1$  to  $5.3 \text{‰}$ , showing evaporation effect on the isotope ratios of larger surface water bodies.

429 On the contrary, mainly at low elevation of the forested area, high d-excess suggests that the  
430 source vapour of the available water was formed from recycled moisture, with d-excess  
431 values ranging from 13.25 to 18.68 ‰. It is for the first time that such depletion in heavy  
432 isotopes of oxygen ( $\delta^{18}\text{O} < -8$  ‰) in water has been observed in South India. Few rainfall  
433 samples obtained at Ooty during the nighttime in November 2013 display  $\delta^{18}\text{O}$  values  
434 between -16 ‰ and -17.9 ‰ (not plotted in Figure 3).

435 <please insert here Fig 3.>

436

#### 437 *4.1. Elevation effect*

438 In general, under the influence of warm tropical climate, the surface and sub-surface water  
439 temperature is close to air temperature,  $26 \pm 2$  °C, for the low to middle elevation (<1500 m  
440 asl). But, in the Nilgiri mountains, as the elevation reaches 2000 m asl, the temperature  
441 decreases rapidly (Table 2). On the summit of the Nilgiris in the Doddabetta peak, spring  
442 water temperature of about 12 °C has been measured during November 2013, and the case of  
443 frost was reported earlier at the meteorological station on the hilltop (Negi, 1996).

444 The  $\delta^{18}\text{O}$  values of water samples from mountainous regions between Arabian Sea coast and  
445 Western Ghats are plotted against the elevation of sampling location to identify the presence  
446 of *elevation effect* on the stable isotope ratios of water (Figure 4). Clearly, two groups of  
447 samples are observed: the first set of samples for elevation below 2050 m asl, with a low  
448 slope ( $-0.09$  ‰/100m,  $R^2 = 0.4$ ) and a second set beyond 2050 m asl with a higher slope ( $-2.5$   
449 ‰/100 m,  $R^2 = 0.7$ ). Table 3 summarizes the reported studies on isotopic elevation effect  
450 from the pioneer works to more focus on tropical areas and Indian terrain.

451 <please insert here Fig 4.>

452 <please insert Table3>

453 The multiple linear regression shows that for the 51 data points reported in Table 1, the  
454 *elevation effect* is very significant ( $R^2 = 0.7$ ,  $p < 0.0001$ ; Table 4) to explain the  $\delta^{18}\text{O}$  values.

455 <please insert Table 4>

456

#### 457 *4.2. Rainfall amount effect*

458 The mean stable isotope ratios of rain water, groundwater and river water in the wettest river  
459 basins (annual rainfall amount of  $5500 \pm 1500$  mm in Swarna and Nethravati basins) of the  
460 Western Ghats in Karnataka was reported to be around  $-3.05 \pm 0.2$  ‰ for  $\delta^{18}\text{O}$  with d-excess  
461 of about  $17.7 \pm 3.1$  ‰ (Tripti et al., 2016). Water samples of Agumbe, the wettest place in  
462 South India as well as along the spatial stretch of the Western Ghats display an average  
463 isotope ratio of about  $-3.14 \pm 0.6$  ‰ for  $\delta^{18}\text{O}$  with d-excess of about  $10.16 \pm 4.7$  ‰  
464 (excluding pond and waterfall; Table 2). The observed stable isotope ratios of groundwater in  
465 the wet locations of the Western Ghats stretch in Karnataka show less depletion of heavy  
466 isotopes in water compared to its coastal track at Udupi and Bakrabail (rain water  $\delta^{18}\text{O} = -$   
467  $2.84 \pm 0.28$  ‰ and d-excess =  $16.5 \pm 2.1$  ‰; Tripti et al., 2016) which receives relatively  
468 lower annual rainfall amount of about  $4000 \pm 500$  mm.

469 The isotope ratios of water samples from the Wayanad plateau, around Sultan Battery, the  
470 wettest place (annual rainfall up to 4000 mm) in Kerala, display mean values of about  $-3.36 \pm$   
471  $0.57$  ‰ for  $\delta^{18}\text{O}$  and  $12.95 \pm 5.06$  ‰ for d-excess (Table 2). This isotopic ratio of  
472 groundwater is relatively lower than that of the long-term mean rainfall ( $\delta^{18}\text{O} = -2.97 \pm 0.73$   
473 ‰ and d-excess =  $10.66 \pm 0.72$  ‰; Warriar et al., 2010) in the corresponding coastal station  
474 of Kozhikode receiving annual rainfall amount of 3000 mm. It can be observed from Figure 5

475 that except the near shore areas like Ezhimala and Thottada, and the inland region close to the  
476 Nilgiri range (Pykara and Doddabetta), all other water sample locations independent of their  
477 annual rainfall, present a mean  $\delta^{18}\text{O}$  value similar to that of the west coast groundwater ( $\delta^{18}\text{O}$   
478 =  $-3.1 \pm 0.3\text{‰}$ ; [Tripti et al., 2016](#)).

479 The multiple linear regression shows that for the 51 points reported in Table 1, the annual  
480 rainfall parameter or *rainfall amount effect* is not significant ( $R^2 = 0.4$ ,  $p = 0.39$ ; Table 4) to  
481 explain the  $\delta^{18}\text{O}$  values.

482

#### 483 *4.3. Continental effect*

484 When the air masses move away from the Arabian Sea towards the inland, until the Western  
485 Ghats mountain belt, there is a significant *continental effect* on stable isotope ratios of water.  
486 The variability in mean  $\delta^{18}\text{O}$  values as a function of distance to the Arabian Sea for nine  
487 sampling regions is plotted in Figure 5. Water samples located close to the sea (distance < 5  
488 km) show  $\delta^{18}\text{O}$  values of about -2 ‰ which then decreases to -3 ‰ towards the inland (i.e., 5  
489 km < distance < 40 km) along the western part of the Western Ghats, including the sample  
490 location on the moderate elevation mountains like Agumbe and Wayanad. Only the water  
491 samples from stations located far away from the sea (distance > 100 km), like the Nilgiris,  
492 display more depleted oxygen isotopes of about -8 ‰.

493 <please insert here Fig 5.>

494 The multiple linear regression shows that for the 51 data points reported in Table 1, the  
495 distance to the sea or *continental effect* is not significant ( $R^2 = 0.56$ ,  $p = 0.18$ ; Table 4) to  
496 explain the  $\delta^{18}\text{O}$  values.

497

#### 498 4.4. Air masses trajectories

499 The results of the HYSPLIT simulations are given in Figure 6. For the stations along the  
500 Arabian Sea coast (Agumbe and Bakrabail) of mid November 2013, there is an influence of  
501 north-east monsoon with *continental effect* at low elevation, and an influence of the Arabian  
502 Sea side is observed at higher elevation. For the lower elevation stations on the Nilgiris (Ooty  
503 and Pykara) of November 19, 2013, the air masses come from the north-east monsoon, with  
504 coastal and maritime effect. For the sampling stations in Doddabetta, Madikeri, Thrissur  
505 (respectively on November 18, December 02 and December 05 during 2013) and Ezhimala  
506 (October 14, 2014), mainly it is the influence of Bay of Bengal with maritime trajectories as  
507 observed in Figure 6. Overall, the sampling was performed under north-east winter monsoon  
508 conditions, with more *continental effects* for mid-November sampling to more maritime  
509 effects for the early December sampling.

510 <please insert here Fig 6.>

511

## 512 5. Discussion

513 In this section, we review the main factors (*elevation, amount and continental effects*)  
514 controlling the water isotope ratios in perspective with the new results obtained for the  
515 Western Ghats mountain belt covering a latitudinal stretch of about 500 km between 10° 30'  
516 N and 14° N in South India.

### 517 5.1. Elevation effect

518 Most of the climatological, ecological, and geophysical studies reported the effect of elevation  
519 on stable isotope ratio of water as *altitude effect* which has been now rephrased as '*elevation*  
520 *effect*' (McVicar and Körner, 2013). The compilation of 68 studies by [Poage and Chamberlain](#)

521 (2001) reports an isotopic lapse rate ranging from -0.10 to -0.51 ‰/100 m asl on  $\delta^{18}\text{O}$  values  
522 (except extreme latitudes, -0.62 to -1.83 ‰/100 m asl), with a mean value of  $-0.28 \pm 0.03$   
523 ‰/100 m asl. In the Himalayas, the isotopic lapse rate ranges between -0.14 ‰/100 m asl on  
524 the Indian slope and up to -0.25 ‰/100 m asl on the Tibetan plateau (Poage and Chamberlain  
525 2001). Limited studies focused on the *elevation effect* in South India. The study on  
526 groundwater isotopes by Deshpande et al. (2003) detected a possible *elevation effect* of -0.4  
527 ‰/100 m asl for  $\delta^{18}\text{O}$  in well water located at an elevation between 400 and 1000 m asl in  
528 Southwest India. But, from the recalculation of slope for the whole set of points located  
529 between Arabian Sea coast and 914 m asl, as displayed in Figure 8a of Deshpande et al.  
530 (2003), the isotopic lapse rate is only -0.11 ‰/100 m asl. Similar values (-0.12 ‰/100 m asl;  
531 Scholl et al., 2009) of isotopic depletion with elevation has been reported for the tropical  
532 coastal forest in Puerto Rico. Recent study on the precipitation across the Pamba River,  
533 Kerala suggest an isotopic lapse rate of about -0.10 ‰/100 m asl (Resmi et al., 2016). Table 3  
534 summarizes the reported studies on isotopic elevation effect from the pioneer works to more  
535 focus on tropical areas and Indian terrain. In Sri Lanka, Edirisinghe et al. (2017) have  
536 reported the isotopic lapse rate of -0.6 ‰/100 m asl for the north-east monsoon, but no value  
537 for the south-west monsoon has been reported as there was no enough rain water collectors on  
538 the south-west of Sri Lanka.

539 In our previous studies (Lambs et al., 2011; Tripti et al., 2016), the sampling along the hill  
540 slopes of Kudremukh, Charmadi Ghats (1300 to 1800 m asl) and Mullayanigiri (1900 m asl;  
541 highest peak of Karnataka) did not show any isotopic *elevation effect*. The data on stable  
542 isotope ratio of water samples from this work show an isotopic lapse rate of -0.09 ‰/100 m  
543 for stations below 2050 m asl which is similar to that reported in other tropical areas (Table  
544 3). But for the region at elevation greater than 2050 m asl in the Western Ghats belt of South  
545 India, a stronger isotopic lapse rate of about -2.5 ‰/100 m asl is found with water highly



546 depleted in heavy isotopes of oxygen ( $\delta^{18}\text{O} = -9.5 \text{ ‰}$ ) as recorded in high mountains of the  
547 Nilgiri ranges at Doddabetta peak. The water samples from the Nilgiri ranges (1950-2300 m  
548 asl) exhibit higher isotopic lapse rate of 1.5 ‰/100 m asl for  $\delta^{18}\text{O}$  whereas the mountains  
549 close to the eastern Arabian Sea like Ezhimala, Agumbe and Chembra exhibit no such  
550 depletion in heavy isotopes of oxygen with elevation (Figure 4). This indicates that there  
551 exists a unique relationship between elevation and stable isotope ratios of surface and sub-  
552 surface water in different mountain ranges of the Western Ghats. When we recalculate the  
553 overall isotopic *elevation effect* from 0 to 2300 m asl, the overall slope value is -0.31 ‰/100  
554 m. The overall isotopic effect observed for the water of the Western Ghats is slightly higher  
555 than the global mean isotopic lapse rate. In the humid tropical areas, the isotopic *elevation*  
556 *effect* on the stable isotope ratios of water is lower (around -0.10 ‰/100 m asl) due to the  
557 moisture contribution from higher air vapour recycling. But when reaching higher elevation of  
558 relatively less humid region, our study reveals that the stable isotope ratios of water are  
559 largely controlled by elevation effect in the Western Ghats mountain belt.

560 Until now, such depletion in heavy isotope ( $^{18}\text{O}$ ) of oxygen ( $-9.5\text{‰} < \delta^{18}\text{O} < -7.3 \text{ ‰}$ , present  
561 study) has not been reported for river and groundwater in the literature for South India,  
562 although the closer values are reported in few studies ([Achyuthan et al., 2010](#); [Hameed et al.,](#)  
563 [2015](#)). Firstly, for the west flowing Chaliyar River, the lowest  $\delta^{18}\text{O}$  reported is -5.30 ‰  
564 ([Hameed et al., 2015](#)) for the water originating at the foothills of the Chembra and Mukurthi  
565 range. Secondly, lower oxygen isotope ratios ( $\delta^{18}\text{O} = -7.7 \text{ ‰}$ ; [Achyuthan et al., 2010](#)) have  
566 been reported for the east flowing Kaveri river near Mettur Dam due to significant  
567 contribution of the tributary flowing from the Nilgiri range. Similar depleted water isotopes  
568 were observed during our sampling in November 2013, where a river in Mule hole basin  
569 display  $\delta^{18}\text{O} = -6.7 \text{ ‰}$  ([Lambs et al., under preparation](#)). All these studies, with oxygen  
570 isotope ratios much lower than -4.5 ‰, indicate a possible depletion of heavy isotopes in

571 water at higher peaks of the Western Ghats with elevation greater than 2000 m asl. For other  
572 east flowing rivers of South India originating in the Western Ghats, higher variability of stable  
573 isotope ratios has been reported, i.e., for the Maheshwaram watershed ( $\delta^{18}\text{O} = -4.7 \text{ ‰}$ ; [Negrel  
574 et al., 2011](#)) and for the Mahanadi and Godavari rivers (respectively  $-6.1 \text{ ‰}$  and  $-5.5 \text{ ‰}$ ;  
575 [Lambs et al., 2005](#)) as they are largely influenced by north-east monsoon.

576 It can be noted that the small isotopic *elevation effect* (less than  $1 \text{ ‰}$  on the  $\delta^{18}\text{O}$  scale)  
577 observed here for the Western Ghats below 2000 m asl is similar to that reported for the cloud  
578 forest where there is a secondary control from strong water vapour recycling process ([Scholl  
579 et al., 2009](#)) with a slope of  $-0.12 \text{ ‰}/100\text{m}$  as given in Table 3. On the contrary, in the same  
580 Arabian Sea coast, further North as well as in the South, higher isotopic *elevation effect* is  
581 found even below 2000 m asl in the drier regions. For instance, the stable isotope  
582 measurements carried out on groundwater in Sri Lanka (north-west and south-west slopes on  
583 the central mountains) and Rajasthan (on the south-west slope of the Aravalli mountain range)  
584 represent an isotopic lapse rate of  $-0.18 \text{ ‰}/100 \text{ m asl}$  (Figure 7; data from [Lambs, under  
585 preparation](#)) for the  $\delta^{18}\text{O}$  values. It is also observed that these water samples display lower  
586 oxygen isotope ratios,  $-8 \text{ ‰} < \delta^{18}\text{O} < -6 \text{ ‰}$  at 1400 m asl.

587 <please insert here Fig 7.>

588 It is also important to consider the possible contribution by isotopic spike effect ([Lambs et al.,  
589 2018](#)) of storm during the north-east monsoon which leads to higher depletion of heavy  
590 isotopes in precipitation water. Compared with normal tropical rainfall, the tropical storms  
591 display distinct depletion of heavy isotopes of oxygen in water. During large tropical storms,  
592 the strong convective effect generates  $^{18}\text{O}$  - depleted rainfall with much lower oxygen isotope  
593 ratios between  $-12$  and  $-8 \text{ ‰}$ , as reported by [Lawrence \(1998\)](#) and more recently by [Lambs et  
594 al. \(2018\)](#). The water samples obtained from inland regions in the Nilgiri ranges during

595 November 17-19, 2013 show an impact from the isotopic spike effect of storms. There was  
596 effectively an extremely severe cyclonic storm named “Phailin” over the Bay of Bengal  
597 during October 04 - 14, 2013, but entered the Indian coast further north-east (in Orissa) of the  
598 sampling sites. At a later stage during November 13 - 17, the storm originating from a strong  
599 depression in the Bay of Bengal entered the Tamil Nadu coast, and during November 18 - 21,  
600 severe cyclone “Helen” made its entry through Andhra Pradesh in South India. The HYSPLIT  
601 simulation (Figure 6) shows effectively that the air mass over the Doddabetta peak had its  
602 original path from the Bay of Bengal more close to the Andaman Island, from where the  
603 cyclone Helen originated. However, the sampled water will not have much influence of storm  
604 from cyclone Helen as samples were collected prior to its first landfall rain over the Indian  
605 coast. The water isotope ratios for the rainfall obtained during this period in the Nilgiri range  
606 were effectively depleted in heavy isotopes with  $\delta^{18}\text{O}$  of about  $-17 \pm 0.9$  ‰ (rain water in  
607 equilibrium with cooler water vapour), but the results are from only few samples ( $n = 2$ ).  
608 Nevertheless, the huge water reservoir in Ooty (the Ooty lake) which covers an area of 3.9  
609  $\text{km}^2$  displays depletion in heavy oxygen isotope with  $\delta^{18}\text{O}$  value of about  $-5.3$  ‰. It is noted  
610 that the water from this lake has a d-excess value of  $-2.1$  ‰ which shows a strong evaporation  
611 of the lake water. This suggests that the original lake water exhibited more depletion of  $^{18}\text{O}$  in  
612 water before undergoing evaporation, certainly similar to the groundwater isotope ratios ( $\delta^{18}\text{O}$   
613  $= -7.3$  ‰) as observed for the Ooty village. This also indicates that the storm effect was  
614 uniform over the Nilgiris and the immediate water sampling displayed a strong elevation  
615 effect in this region of the Western Ghats. Thus, it is important to note that along with the  
616 northeast monsoon influence, the earlier storms from cyclone Phailin and Bay of Bengal  
617 depression had an effective contribution towards the surface water and sub-surface water in  
618 the Nilgiris. This has led to lower water isotope ratios at higher elevations inland compared to  
619 the coastal groundwater along the eastern Arabian Sea side. The study determines that the

620 water from the higher mountains of the Western Ghats depicts the global elevation effect soon  
621 after the strong influence of the monsoon and much before the dominance of secondary  
622 processes like evaporation and contribution of recycled vapours from evapo-transpiration.  
623 This reveals that the time scale of observation plays a major factor (Poage and Chamberlain,  
624 2001) in monitoring the relationship between elevation and stable isotope ratios of surface and  
625 sub-surface water in the Western Ghats mountain belt.

626

### 627 *5.2. Rainfall amount effect*

628 The highest rainfall (21.32 mm/day; Tawde and Singh, 2015) in South India during summer  
629 monsoon season is observed over windward side of the Western Ghats mountain range in  
630 Karnataka, centered at 13° 13' N latitude, close to Udupi. The variability in monsoonal  
631 rainfall (Figure 1.d.) with changing longitude (west-east direction) and latitude (south- north  
632 direction) i.e., across and along the Western Ghats (Gunnell, 1997) corresponds to the  
633 topographic structures of the mountain barriers and the contribution from seasonal monsoon  
634 sources. It is reported that the maximum rainfall due to orography of the Western Ghats  
635 during summer monsoon season is on an average 50 km before the highest peak and  
636 corresponds to an elevation of about 600 m asl, beyond that the rainfall decreases (Tawde and  
637 Singh, 2015). It is at this middle elevation that the wettest places are found in Karnataka  
638 (Hulikal at 13° 43' N and Agumbe at 13° 30' N) and in Kerala (Vythiri on the edge of the  
639 Wayanad plateau at 11° 33' N and Walakkad in the Silent Valley at 11° 03' N).

640 Tropical coastal areas are typically characterized by rain water with  $\delta^{18}\text{O}$  of about  $-3 \pm 1$  ‰  
641 (GNIP database) and the groundwater of several tropical coasts and islands reflect similar  
642 mean  $\delta^{18}\text{O}$  values (Lambs et al., 2016, 2018). This is also the case for the west coast of South  
643 India, with similar groundwater stable isotope ratios at Udupi ( $\delta^{18}\text{O} = -3.09 \pm 0.05$  ‰, n=34;

644 [Tripti et al., 2016](#)). This  $\delta^{18}\text{O}$  value corresponds with the rainfall mean weighted values in the  
645 nearest GNIP station, Kozhikode ( $\delta^{18}\text{O} = -2.97 \pm 0.73 \text{ ‰}$ ; [Warrier et al., 2010](#)). Only the  
646 water from the eastern part of South India which is mainly influenced by the north-east winter  
647 monsoon and higher *continental effect* display lower isotope ratios ( $\delta^{18}\text{O} = -6 \text{ ‰}$ ; [Deshpande](#)  
648 [et al., 2003](#)).

649 In this study, the mean oxygen isotope ratios of water at sampling stations of Agumbe ( $\delta^{18}\text{O} =$   
650  $-2.95 \pm 0.66 \text{ ‰}$ ;  $n = 6$ ), Bakrabail ( $\delta^{18}\text{O} = -3.05 \pm 0.34 \text{ ‰}$ ;  $n = 5$ ) and Thrissur ( $\delta^{18}\text{O} = -$   
651  $3.11 \text{ ‰}$ ) are very similar, although these stations received contrasting annual rainfall amount  
652 from 6000 mm (Agumbe) to 3000 mm (Thrissur). Similar case is found further south between  
653 the Wayanad plateau around Sultan Bathery (mean groundwater  $\delta^{18}\text{O} = -3.1 \pm 0.5 \text{ ‰}$ ) and the  
654 relative drier coastal station at Kozhikode ( $\delta^{18}\text{O} = -2.97 \pm 0.73 \text{ ‰}$ ; [Warrier et al., 2010](#)). All  
655 these sampling stations confirm the low *rainfall amount effect* on the water isotopic ratio  
656 along the spatial stretch of the Western Ghats belt.

657 The study on stable isotope ratios ( $\delta^{18}\text{O}$  and  $\delta^2\text{H}$ ) of groundwater, surface water and rainfall  
658 from coast to inland in south-west of Karnataka shows weaker *rainfall amount effect* on the  
659 water isotope ratios due to the influence of higher continental vapour recycling process (as  
660 represented by higher d-excess values of about 15 ‰) in the two humid tropical basins of the  
661 Western Ghats ([Tripti et al., 2016](#)). On the contrary, a reversed *rainfall amount effect* on the  
662  $\delta^{18}\text{O}$  variability was observed for the precipitation over Mangalore ([Yadava et al., 2007](#)),  
663 although they still show a weaker *rainfall amount effect* within the monsoonal months. At  
664 Kunnamangalam, 12 km inland of Kozhikode (Kerala), the study by [Warrier et al. \(2010\)](#)  
665 shows a poor correlation between rainfall amount and  $\delta^{18}\text{O}/\delta^2\text{H}$  values over the three years  
666 period from 2005 to 2007. The authors stated that the region receives a continuous supply of  
667 moist air masses as the south-west monsoon currents move across extended marine regions

668 before reaching Kozhikode. In addition, the study on the  $\delta^{18}\text{O}$  variability in precipitation  
669 along the Kerala stretch suggests the influence of large-scale convection and cloud spread  
670 (Lekshmy et al., 2014) rather than the *rainfall amount effect*. Recent studies (Hameed et al.,  
671 2016; Resmi et al., 2016) on the spatial variability of stable isotope ratios ( $\delta^{18}\text{O}$  and  $\delta^2\text{H}$ ) of  
672 precipitation over the Kerala region also support weaker *rainfall amount effect* and have  
673 attributed it to the steady state supply of moisture and also vapour recycling over the  
674 continent. Thus, the water in the west coast and along moderate elevations of the Western  
675 Ghats stretch in South India does not display a high correlation between the stable isotope  
676 ratios of water and precipitation amount.

677

### 678 5.3. Continental and seasonal effects

679 As stated in the previous section, precipitation (rain water) along the tropical coasts display  
680  $\delta^{18}\text{O}$  value of about  $-3 \pm 1$  ‰ (GNIP database) and represents relative depletion of heavy  
681 isotopes than that of the seawater ( $\delta^{18}\text{O} = 0$  ‰, by definition). The two GNIP stations in  
682 South India, Kozhikode and Tirunelveli (Figure 1.b.) display very similar weighted mean  
683  $\delta^{18}\text{O}$  values of about  $-2.97$  and  $-2.79$  ‰ respectively. In our earlier studies (Lambs et al.,  
684 2011; Tripti et al., 2013, 2016), it was reported that there is a homogeneity in the groundwater  
685 isotopic signature from coastal plain up to the moderate elevation ( $< 1500$  m asl) of the Ghats.  
686 The mean value of  $\delta^{18}\text{O}$  in water samples was around  $-3.15 \pm 0.63$  ‰, close to the GNIP  
687 rainwater  $\delta^{18}\text{O}$  value ( $-2.97$  ‰) of Kozhikode (Figure 1.b.). Only the coastal stations adjacent  
688 to the Arabian Sea, like the groundwater in the estuarine zone of the Swarna River at Hude  
689 displayed enrichment of heavy isotopes with  $\delta^{18}\text{O}$  value of about  $-2.26$  ‰ (Tripti et al., 2016).

690 In this study, the costal stations of Ezhimala and Thottada which receive directly the sea  
691 moisture display respectively,  $\delta^{18}\text{O} = -1.92 \pm 0.55$  ‰ (n=8) and  $\delta^{18}\text{O} = -2.31 \pm 0.74$  ‰

692 (n = 8). Further inland, the groundwater at low elevation stations show a homogenous  
693 groundwater with  $\delta^{18}\text{O}$  around -3 ‰. This is clearly represented in Figure 5, where the water  
694 isotope ratios ( $\delta^{18}\text{O}$ ) vary between -2.95 ‰ and -3.36 ‰, except for the sample stations of  
695 Ezhimala and Thottada. This represents that for the region stretching to about 500 km distance  
696 along the Western Ghats i.e., from Udipi (Karnataka) to Thrissur (Kerala), the groundwater  
697 and surface water display a similar oxygen isotope ratio ( $\delta^{18}\text{O}$ ) of about  $-3.0 \pm 0.5$  ‰, before  
698 any evaporation. It is interesting that water homogeneity extends till 50 to 70 km inland,  
699 including moderately elevated plateaus like Agumbe, Madikeri and Wayanad of the Western  
700 Ghats. The higher moisture availability and the thick vegetation cover favour higher  
701 continental vapour recycling in this region. The higher continental moisture recycling in the  
702 western part of the Western Ghats and the uniform distribution of recycled moisture over the  
703 short distance led to homogenous signatures in the stable isotope ratios of groundwater (Tripti  
704 et al. 2016). However, there is a shift in this homogeneity further inland, extending beyond  
705 100 km from the Arabian Sea coast, at higher elevations in the Western Ghats with  
706 groundwater exhibiting higher depletion of heavy isotopes ( $\delta^{18}\text{O} = -7.0 \pm 1.5$  ‰) as observed  
707 for the Nilgiri ranges. The water in this inland region exhibited colder temperature relative to  
708 that of the coastal and moderate elevation stations in the Western Ghats. In addition, these  
709 inland stations receive relatively higher north-east monsoon precipitation than the west coast,  
710 and thus, the surface water and sub-surface water are recharged with more continental rainfall  
711 characterized by water with higher depletion of heavy isotopes.

712

#### 713 *5.4. Variability of deuterium-excess*

714 There is a higher variability of d-excess in the surface and subsurface water of the Western  
715 Ghats with mean values ranging from + 6.5 to + 13.42 ‰. The plot (Figure 8) of d-excess as a

716 function of distance from the coastline and elevation displays a lower increasing trend unlike  
717 that of the global water (Bershaw, 2018) associated either with source moisture mixing or  
718 sub-cloud evaporation. The calculated d-excess ranges between 3 ‰ and 20 ‰. The observed  
719 d-excess variability in this humid tropical region corresponds to that reported in the Jeju  
720 Island, Korea and northeast Asia (Lee et al., 2003). However, the d-excess variability  
721 observed in this study corresponds less to the seasonal moisture source contribution as the  
722 west coast samples which are dominated by precipitation input from hot humid tropical  
723 marine air mass from Arabian Sea exhibit higher values and a larger range of d-excess. This is  
724 mainly dependent on the degree of regional continental moisture recycling process and  
725 distribution of the recycled vapours (Tripti et al., 2016) influencing the incoming marine  
726 source moisture along the eastern Arabian Sea coast of India.

727 <please insert here Fig. 8>

728

### 729 5.5. Statistical analysis

730 Multiple linear regression analysis was carried out for determining the extent to which the  
731 *elevation effect*, *continental effect* and *rainfall amount effect* influence the  $\delta^{18}\text{O}$  values. When  
732 running the statistical test for the whole set of points ( $n = 51$ ), the *elevation effect* appears to  
733 be the most significant explicative parameter, and the influence of two other effects remain  
734 insignificant. If we split the dataset into two groups, like in Figure 4, for the first 42 points  
735 with elevation lower than 2050 m asl (Table 4), there is neither a strong nor a significant  
736 contribution from one specific parameter. It is a global contribution which enables  
737 observation of the  $\delta^{18}\text{O}$  values to decrease from -2 ‰ along the eastern coast of Arabian Sea  
738 to -4.0‰ more inland at 1800 m asl in the Western Ghats. For the last 9 points, i.e. above  
739 2050 m asl, the *elevation effect* and the *rainfall amount effect* become significant ( $R^2 = 0.77$ , p



740 < 0.1 and  $R^2 = 0.81$ ,  $p < 0.05$  respectively) in controlling stable isotope ratios of water at high  
741 elevation of the Western Ghats. This suggests that for the tropical mountains of high elevation  
742 and with less relative humidity, the lower isotopic ratios of surface water and sub-surface  
743 water were characteristics of deep cooling due to high orographic upliftment of seasonal air  
744 moisture, severe storm effect and higher annual rainfall input.

745

#### 746 *5.6. Implications of stable isotopes of water in the Western Ghats mountain belt*

747 This study and the earlier reported work (Lambs et al., 2011; Tripti et al., 2013, 2016) suggest  
748 that in the tropical monsoon climate region of the Western Ghats, the high water vapour  
749 recycling is due to higher precipitation, warmer temperature, wetlands and large vegetation  
750 cover (around 40% of forest). The higher moisture input ( $\sim 2000$  mm < annual precipitation <  
751 6000 mm; Figure 1.b.) from the nearby oceanic source coupled with suitable temperature (i.e.,  
752  $\sim 20 < t < 30^\circ$  C) and land-use/land cover (i.e., vegetation) in the continent supports high  
753 relative air humidity (75-100 %) which triggers higher vapour recycling (Breitenbach et al.,  
754 2010) in this region. This indicates the dominance of terrestrial moisture recycling process  
755 over the Western Ghats rather than the Rayleigh distillation process of moisture from oceanic  
756 source. This is reflected by the higher stable isotope ratios of water over the continent leading  
757 to less depletion of heavy isotopes ( $\sim \delta^{18}\text{O} = -3$  ‰) and higher d-excess values ( $\sim 15$  ‰) for  
758 the wetter regions of west coast. However, the effect of vapour recycling on the isotopic  
759 signature of incoming moisture becomes less dominant in the region where the moisture input  
760 is relatively minimal ( $\sim$  annual precipitation < 2000 mm) from the summer monsoon mainly  
761 due to the rain shadow effect. However, these inland regions exhibit relatively cooler  
762 temperature (i.e.,  $T < 20^\circ$  C) due to high air lifting and contribution from north-east monsoon.  
763 There is a higher reflection of original moisture source and the mixing process on the stable

764 isotope ratios of water in such semi-arid tropical regions. Thus, a clear indication of Rayleigh  
765 distillation or *elevation effect* is observed on the isotopic signatures of moisture which in turn  
766 leads to more depletion of heavy isotopes ( $\sim \delta^{18}\text{O} < - 6\text{‰}$ ) in water present in inland regions.  
767 This shows that the continental vapour recycling process and their role in controlling moisture  
768 flux (Froehlich et al., 2002; Risi et al., 2013; Sturm et al., 2007) are important factors even in  
769 the humid coastal regions receiving higher precipitation. Although there could be several  
770 factors that control the moisture isotopic signatures and their subsequent reflection in the  
771 groundwater and surface water, this study shows that temperature coupled with higher  
772 seasonal moisture input (mainly precipitation amount) and vegetation cover play a significant  
773 role in governing the stable isotope ratios of water over the regional scale and the subsequent  
774 water cycle over the highlands of the Western Ghats mountain belt in India. Also, it is  
775 important to note that the stable isotopes of water show homogenous signature up to moderate  
776 elevation (i.e., 2000 m asl) for the humid tropical mountains, and the isotopic *elevation effect*  
777 is observed only in the mountains of elevation greater than 2000 m asl of the Western Ghats.  
778 The findings of this study are significant as it has implications on the studies involving past  
779 climate and paleoelevation of the tropical mountain belt using records preserved in  
780 paleoarchives. This will help in improving the understanding of isotopic signatures of  
781 paleowater, tree ring, speleothem and other geological records found in South India. With less  
782 GNIP observations stationed in South India, the present study (though the observation is  
783 mainly from surface and subsurface water) adds to the global database, as it provides the new  
784 evidence on the isotopic *elevation effect* along the highlands of tropical mountain rainforest  
785 ecosystem of India. This also has larger implications on the hydrological and Indian  
786 monsoonal climatic systems, and further helps in the sustainable water resource management  
787 of South India.

788

## 789 6. Conclusions

790 Humid tropical mountains display a lower isotopic *elevation effect* due to limited temperature  
791 gradient, high relative humidity, evergreen forest evapotranspiration and high water vapour  
792 recycling. The Western Ghats mountain belt of South India has similar characteristics, and as  
793 such the stable isotope ratios of rainfall and water bodies exhibits lower variability with  
794 elevation up to 2000 m asl with a mean oxygen isotope ratio ( $\delta^{18}\text{O}$ ) of about  $-2.5 \pm 0.5$  ‰ and  
795 a limited seasonal effect (maximum difference in mean  $\delta^{18}\text{O}$  between seasons is  $\pm 0.5$  ‰ for  
796 larger river basins and  $\pm 0.2$  ‰ for smaller basins). The homogeneity in the ground water  
797 isotope ratio along the western coastal plain from Udupi to Thrissur in South India is  
798 explained by the wide-scale marine moisture distribution from the dominant south-west  
799 summer monsoon system. The moisture characteristics on the foothills of the Western Ghats  
800 are more affected by the water vapour recycling as observed from the higher d-excess (around  
801 15 ‰), particularly in the vegetation covered and wetland regions.

802 The present study reveals for the first time that beyond 2000 m asl in the Western Ghats, such  
803 as in the Nilgiri ranges, the surface and subsurface water exhibit relatively lower stable  
804 isotope ratios with  $\delta^{18}\text{O}$  values ranging from  $-5.3$  ‰ for the lake to  $-9.5$  ‰ for the springs and  
805 open wells of hills at higher elevation. This reflects a very strong isotopic *elevation effect* ( $1.8$   
806 ‰/100 m for  $\delta^{18}\text{O}$ ) for the water from the Western Ghats mountain belt between 2000 and  
807 2600 m asl where the cold air temperature (i.e., 10 - 20 °C) prevails. The water contribution  
808 from the recycled vapours masks the strong effect of elevation, rainfall amount and  
809 continental effect on water isotope ratios under the following conditions: i) when there is an  
810 increased availability of terrestrial moisture to undergo secondary processes like recycling and  
811 evaporation, and ii) after the vapours from short severe storm effect recedes. As the Western  
812 Ghats mountain belt forms the source of major South Indian Rivers and provides a platform  
813 for the dual monsoon system observation, this study has a global implication with a new

814 understanding on the dynamic role of tropical mountains in monitoring the humid climatic  
815 system, the Indian monsoon and regional hydrology of South India. The monsoon arrival and  
816 its interannual variability affect numerous people living in these fertile mountain ranges, and  
817 in the context of global climate change, emphasize the sensitive response of these tropical  
818 mountains to anthropogenic influences. Thus, a minor change in the land use/land cover (such  
819 as deforestation, agricultural activities and urbanization) and topography of the Western Ghats  
820 can have a significant impact on the degree of atmospheric moisture feedback mechanisms  
821 and is directly reflected by the climatic conditions of tropical monsoon forest ecosystem in  
822 India.

823

#### 824 **Acknowledgements**

825 This work was funded by the International Unit of Toulouse III University (Toulouse,  
826 France). We thank Dr. Balakrishna K and Manipal Academy of Higher Education (earlier  
827 Manipal University), Manipal for the Structured PhD fellowship of TM during November  
828 2013, Dr. Ajitkumar MP for assistance during the field work at Kannur, and the Associate  
829 Editor and three anonymous reviewers for their critical comments and constructive  
830 suggestions on the earlier version of manuscript. We are thankful to NOAA Air Resources  
831 Laboratory for accessibility to HYSPLIT Trajectory model. We also acknowledge Indian  
832 National Science Academy (INSA), Government of India for the DST-INSPIRE Faculty  
833 award to TM and sponsoring the present research on the Western Ghats.

834

#### 835 **In Memoriam**

836 We dedicate this work to our esteemed colleague, Dr. C. Unnikrishnan Warriar, former Head  
837 of Isotope Hydrology Divison, Centre for Water Resources Development and Management,  
838 Kozhikode, Kerala. He passed away untimely in a tragic road accident during October 2017.  
839 He initiated the monitoring of rainfall for isotopic composition in 2004 at Kunnamangalam,  
840 Kozhikode the data which was subsequently included in the GNIP-data base.

841 We also dedicate our work to Dr. R. Ramesh, Professor (rtd.), Geosciences Division, Physical  
842 Research Laboratory, Ahmedabad and National Institute of Science Education and Research,  
843 Bhubaneswar. He passed away during April 2018. He was one of the meritorious researchers  
844 in India in implementing stable isotope techniques to address multidisciplinary questions in  
845 the field of Earth Sciences.

846 Their contributions in the field of stable isotopes provide strong base for future research.

847

## 848 **References**

849 Achyuthan, H.M., Michelini, M., Sengupta, S.D., Kale, V.S., Stenni, B., Flora O., 2010.  
850 Oxygen and hydrogen isotopic characteristics of the Kaveri river surface waters, southern  
851 peninsular, India. IAEA report, ICTP, IC/2010/103.

852 Aggarwal, P.K., Alduchov, O.A., Froehlich, K.O., Araguas-Araguas, L.J., Sturchio, N.C.,  
853 Kurita, N., 2012. Stable isotopes in global precipitation: A unified interpretation based on  
854 atmospheric moisture residence time. Geophysical Research Letters 39, L11705.

855 Araguás-Araguás, L.J., Froehlich, K.O., Rozanski, K., 2000. Deuterium and oxygen-18  
856 isotope composition of precipitation and atmospheric moisture. Hydrological Processes 14,  
857 1341-1355.

858 Bershaw, J., 2018. Controls on deuterium excess across Asia. Geosciences 8, 257.

859 Biasutti, M., Yuter, S.E., Burleyson, C.D., Sobel A.H., 2012. Very high resolution rainfall  
860 patterns measured by TRMM precipitation radar: Seasonal and diurnal cycles. *Climate*  
861 *Dynamics* 39, 239-258.

862 Bowen G.J., 2008. Spatial analysis of the intra-annual variation of precipitation isotope ratios  
863 and its climatological corollaries. *Journal of Geophysical Research* 113, D05113.

864 Bowen, G.J., Revenaugh, J., 2003. Interpolating the isotopic composition of modern meteoric  
865 precipitation. *Water Resources Research* 39, 1299, 9.1-9.13.

866 Breitenbach, S.F.M., Adkins, J.F., Meyer, H., Marwan, N., Kumar, K.K., Haug, G.H., 2010.  
867 Strong influence of water vapor source dynamics on stable isotopes in precipitation observed  
868 in Southern Meghalaya, NE India. *Earth and Planetary Science Letters* 292, 212-220.

869 Chamberlain, C.P., Poage M.A., 2000. Reconstructing the paleotopography of mountain belts  
870 from the isotopic composition of authigenic minerals. *Geology* 28, 115-118.

871 Clark, I.D., Fritz, P., 1997. *Environmental isotopes in hydrogeology*, Lewis Publishers, New  
872 York, 328.

873 Coplen, T.B., 2011. Guidelines and recommended terms for expression of stable-isotope-ratio  
874 and gas-ratio measurement results. *Rapid Communications in Mass Spectrometry* 25, 2538-  
875 2560.

876 Craig, H., 1961. Isotopic variations in meteoric waters. *Science* 133, 1702-1703.

877 Dansgaard, W., 1964. Stable isotopes in precipitation. *Tellus* 16, 436-468.

878 Day, J.A., Fung, I., Rissi, C., 2015. Coupling of South and East Asian Monsoon precipitation  
879 in July-August. *Journal of Climate* 28, 4330-4356.

880 Deshpande, R.D., Bhattacharya, S.K., Jani, R.A., Gupta, S.K., 2003. Distribution of oxygen  
881 and hydrogen isotopes in shallow groundwaters from Southern India: influence of a dual  
882 monsoon system. *Journal of Hydrology* 271, 226-239.

883 Dinçer, T., Payne, B.R., Florkowski, T., Martinec, J., Tongiorgi, E.G.E.I., 1970. Snowmelt  
884 runoff from measurements of tritium and oxygen-18. *Water Resources Research* 6, 110-124.

885 Edirisinghe, E.A.N.V., Pitawala, H.M.T.G.A., Dharmagunawardhane, H.A., Wijayawardane,  
886 R.L., 2017. Spatial and temporal variation in the stable isotope composition ( $\delta^{18}\text{O}$  and  $\delta^2\text{H}$ ) of  
887 rain across the tropical island of Sri Lanka. *Isotopes in Environmental Health Studies* 53, 628-  
888 645.

889 Epstein, S., Mayeda, T., 1953. Variation of  $\text{O}^{18}$  content of water from natural sources.  
890 *Geochimica et Cosmochimica Acta* 4, 213-214.

891 Friedman, I., Redfield, A.C., Schoen, B., Harris, J., 1964. The variation of the deuterium  
892 content of natural waters in the hydrologic cycle. *Reviews of Geophysics* 2, 177-224.

893 Froehlich K., Rozanski K., Araguas-Araguas L. 1998. Isotope hydrology: applied discipline in  
894 Earth sciences. In Causse C. and Gasse F. (eds.) *Hydrologie et géochimie isotopique*. Paris,  
895 Orstom, 55-72.

896 Froehlich, K., Gibson, J., Aggarwal, P.K., 2002. Deuterium excess in precipitation and its  
897 climatological significance (IAEA-CSP-13/P), International Atomic Energy Agency, 54-66.

898 Garcia, M., Villalba, F., Araguas-Araguas, L., Rozanski, K., 1998. The role of atmospheric  
899 circulation patterns in controlling the regional distribution of stable isotope contents in  
900 precipitation: Preliminary results from two transects in the Ecuadorian Andes. In: *Isotope*  
901 *Techniques in the Study of Environmental Change*, International Atomic Energy Agency,  
902 Vienna, 127-140.

903 Gat, J.R., 1996. Oxygen and hydrogen isotopes in the hydrological processes. *Hydrology and*  
904 *Earth System Sciences* 24, 225-262.

905 Gonfiantini, R., Roche, M.A., Olivry, J.C., Fontes, J.C., Zuppi, G.M., 2001. The altitude  
906 effect on the isotopic composition of tropical rains. *Chemical Geology* 181, 147-167.

907 Gunnell, Y., 1997. Relief and climate in South Asia: the influence of the Western Ghats on  
908 the current climate pattern of peninsular India. *International Journal of Climatology* 17, 1169-  
909 1182.

910 Gunnell, Y., 1998. Passive margin uplifts and their influence on climatic change and  
911 weathering patterns of Tropical shield regions. *Global Planetary Change* 18, 47-57.

912 Gurumurthy, G.P., Balakrishna, K., Tripti, M., Riotte, J., Audry, S., Braun, J.J., Lambs, L.,  
913 Udaya Shankar, H.N., 2015. Sources and processes affecting the chemistry of subsurface  
914 waters along a tropical river basin, Southwestern India. *Environ. Earth Sci.* 73, 333-346.

915 Hameed, A.S., Resmi, T.R., Suraj, S., Warriar, C. U., Sudheesh, M., Deshpande R.D., 2015.  
916 Isotopic characterization and mass balance reveals groundwater recharge pattern in Chaliyar  
917 river basin, Kerala, India. *Journal of Hydrology: Regional Studies* 4, 48-58.

918 Hameed, A.S., Resmi, T.R., Praveenbabu, M., Sudheesh, M., Deshpande, R.D., 2016.  
919 Synoptic variation of stable isotopes in precipitation and ground level vapour in a humid  
920 tropical region, Kerala, India. *Environmental Earth Sciences* 75, 1412.

921 Hobson, K. A., Anderson, R.C, Soto, D.X., Wassenaar, L.I., 2012. Isotopic evidence that  
922 dragonflies (*Pantala flavescens*) migrating through the Maldives come from the northern  
923 Indian subcontinent. *PLOS One* 7, e52594, pp. 1-4.

924 Jain, S.K., Agarwal, P.K., Singh, V.P., 2007. *Hydrology and water resources of India*. Series:  
925 *Water science and technology library*, Springer, 57, 1260.



926 Kaseke, K.F., Wang, L., Wanke, H., Turewicz, V., Koeniger, P., 2018. An analysis of  
927 precipitation isotope distribution across Namibia using historical data. PLOS One 11,  
928 e0154598.

929 Kendall, C., McDonnell J.J., 1993. Effect of intrastorm isotopic heterogeneities of rainfall, soil  
930 water, and groundwater in runoff modeling. In: *Tracers in Hydrology, Proceedings of the*  
931 *Yokohama Symposium*, 41-48. Publication 215, International Association of Hydrological  
932 Sciences, Wallingford.

933 Kumar, B., Athavale, R.N., Sahay, K.S.N., 1982. Stable isotope geohydrology of the lower  
934 Maner basin, Andhra Pradesh, India. *Journal of Hydrology* 59, 315-330.

935 Lachniet, M.S., Patterson, W.P., 2002. Stable isotope values of Costa Rican surface waters.  
936 *Journal of Hydrology* 260, 135-150.

937 Lachniet, M.S., Patterson, W.P., 2006. Use of correlation and stepwise regression to evaluate  
938 physical controls on the stable isotope values of Panamanian rain and surface waters. *Journal*  
939 *of Hydrology* 324, 115-140.

940 Lachniet, M.S., Patterson, W.P., 2009. Oxygen isotope values of precipitation and surface  
941 waters in northern Central America (Belize and Guatemala) are dominated by temperature  
942 and amount effects. *Earth and Planetary Science Letters* 284, 435-446.

943 Lambs, L., Balakrishna, K., Brunet, F., Probst, J.L., 2005. Oxygen and hydrogen isotopic  
944 composition of major Indian rivers: a first global assessment. *Hydrological Processes* 19,  
945 3345-3355.

946 Lambs, L., Bompoy, F., Dulormne, M., 2018. Using isotopic spike from tropical storm to  
947 understand water exchange on large scale: case study of Rafael storm in the Lesser Antilles  
948 archipelago. *Rapid Communications in Mass Spectrometry* 32, 457-468.

949 Lambs, L., Gurumurthy, G.P., Balakrishna, K., 2011. Tracing the sources of water using  
950 stable isotopes: first results along the Mangalore-Udupi region, south-west coast of India.  
951 *Rapid Communications in Mass Spectrometry* 25, 2769-2776.

952 Lambs, L., Mangion, P., Mougin, E., Fromard, F., 2016. Water cycle and salinity dynamics in  
953 the mangrove forests of Europa and Juan de Nova Islands, southwest Indian Ocean. *Rapid*  
954 *Communications in Mass Spectrometry* 30, 311-320.

955 Lawrence, J.R., 1998. Isotopic spikes from tropical cyclones in surface waters: opportunities  
956 in hydrology and paleoclimatology. *Chemical Geology* 144, 153-160.

957 Lee, K-S., Grundstein, A.J., Wenner, D.B., Choi, M-S., Woo, N-C., Lee, D-H., 2003.  
958 Climatic controls on the stable isotopic composition of precipitation in Northeast Asia.  
959 *Climate Research* 23, 137-148.

960 Li, C., Yanai, M., 1996. The onset and interannual variability of the Asian Summer Monsoon  
961 in relation to land-sea thermal contrast. *Journal of Climate* 9, 358-375.

962 McDonnell, J.J., Beven, K., 2014. Debates-the future of hydrological sciences: A (common)  
963 path forward? A call to action aimed at understanding velocities, celerities and residence time  
964 distributions of the headwater hydrograph. *Water Resources Research* 50, 5342-5350.

965 McGuire, K., McDonnell, J.J., 2007. Stable isotope tracers in watershed hydrology. In: K.  
966 Lajtha and R. Michener (eds.), *Stable isotopes in ecology and environmental science*, 2nd  
967 editions, Blackwell Publishing, Oxford, UK, 334-374.

968 McVicar, T.R., Körner, C., 2013. On the use of elevation, altitude and height in the ecological  
969 and climatological literature. *Oecologia* 171, 335-337.

970 Mooley, D.A., Shukla, J., 1987. Variability and forecasting of the summer monsoon rainfall  
971 over India. In: C. P. Chang and T. N. Krishnamurti (eds.) Monsoon Meteorology, Oxford  
972 University Press, pp. 26-59.

973 Negi, S.S., 1996. Biosphere reserves in India: land use, biodiversity and conservation. Indus  
974 publication, Delhi, 221 pages.

975 Negrel, P.H., Pauwels, H., Dewandel, B., Gandolfi, J.M., Mascré, C., Ahmed, S. 2011.  
976 Understanding groundwater systems end their functioning through the study of stable water  
977 isotopes in a hard-rock aquifer (Maheswaram watershed, India). Journal of Hydrology 397,  
978 55-70.

979 Pimm, S.L., Sugden, A.M., 1994. Tropical diversity and global change. Science 263, 933-934.

980 Poage, M.A., Chamberlain, C.P., 2001. Empirical relationships between elevation and the  
981 stable isotope composition of precipitation and surface waters: considerations for studies of  
982 paleoelevation change. American Journal of Science 301, 1-15.

983 Rahul, P., Ghosh, P., Bhattacharya, S.K., 2016. Rainouts over the Arabian Sea and Western  
984 Ghats during moisture advection and recycling explain the isotopic composition of Bangalore  
985 summer rains. Journal of Geophysical Research 6148-6163.

986 Ramachandra, T.V., Vinay, D., Bharath, H.A., 2016. Environmental flow assessment in a  
987 lotic ecosystem of central Western Ghats, India. Hydrology Current Research 7, 1-14.

988 Resmi, T.R., Sudharma, K.V., Hameed, A.S., 2016. Isotope characteristics of precipitation in  
989 the Pamba river basin, Kerala, India. Journal of Earth System Sciences 125, 1481-1493.

990 Risi, C., Noone D., Frankenberg, C., Worden J., 2013. Role of continental recycling in  
991 intraseasonal variations of continental moisture as deduced from model simulations and water  
992 vapor isotopic measurements. Water Resources Research 49, 4136-4156.

993 Rozanski, K., Araguás-Araguás, L., Gonfiantini, R., 1992. Relation between long-term trends  
994 of oxygen-18 isotope composition of precipitation and climate. *Science* 258, 981-985.

995 Rozanski, K., Araguás-Araguás, L., Gonfiantini, R., 1993. Isotopic patterns in modern global  
996 precipitation. *Geophysical Monograph Series* 78, 1-36.

997 Sánchez-Murillo R., Birkel C., Welsh K., Esquivel-Hernández, G., Corrales-Salazar, J., Boll,  
998 J., Brooks, E., Roupsard, O., Sáenz-Rosales, O., Katchan, I., Arce-Mesén, R., Soulsby, C.,  
999 Araguás-Araguás, L.J. 2016. Key drivers controlling stable isotope variations in daily  
1000 precipitation of Costa Rica: Caribbean Sea versus Eastern Pacific Ocean moisture sources.  
1001 *Quaternary Science Reviews* 131, 250-261.

1002 Scholl, M.A., Shanley, J.B., Zegarra, J.P., Coplen, T.B., 2009. The stable isotope amount  
1003 effect: new insights from NEXRAD echo tops, Luquillo Mountains, Puerto Rico. *Water  
1004 Resources Research* 45, W12407.

1005 Siegenthaler, U., Oeschger, H., 1980. Correlation of  $^{18}\text{O}$  in precipitation with temperature  
1006 and altitude. *Nature* 285, 314-317.

1007 Sklash, M.G., 1990. Environmental isotope studies of storm and snowmelt runoff generation.  
1008 In: M.G. Anderson and T.P. Burt (eds.), *Process studies in Hillslope Hydrology*, John Wiley  
1009 and Sons, Chichester, UK, pp. 401-435.

1010 Stumpp, C., Klaus, J., Stichler, W., 2014. Analysis of long-term stable isotopic composition  
1011 in German precipitation. *Journal of Hydrology* 517, 351-61.

1012 Sturm, C., Hoffmann, G., Langmann, B., 2007. Simulation of the Stable Water Isotopes in  
1013 Precipitation over South America: Comparing Regional to Global Circulation Models. *Journal  
1014 of Climate* 20, 3730-3750.

1015 Tawde, S.A., Singh, C., 2015. Investigation of orographic features influencing spatial  
1016 distribution of rainfall over the Western Ghats of India using satellite data. *International*  
1017 *Journal of Climatology* 35, 2280-2293.

1018 Tripti, M., Lambs, L., Otto, T., Gurumurthy, G.P., Teisserenc, R., Moussa, I, Balakrishna, K.,  
1019 Probst, J.L., 2013. First assessment of water and carbon cycles in two tropical coastal rivers of  
1020 south-west India - an isotopic approach. *Rapid Communications in Mass Spectrometry* 27,  
1021 1681-1689.

1022 Tripti, M., Lambs, L., Gurumurthy, G.P., Moussa, I., Balakrishna, K., Chadaga, M.D., 2016.  
1023 Water circulation and governing factors in humid tropical river basins in the central Western  
1024 Ghats, Karnataka, India. *Rapid Communications in Mass Spectrometry* 30, 175-190.

1025 UNESCO, 2012. World Heritage list for Western Ghats, ID No. 1342 Rev,  
1026 <http://whc.unesco.org/en/list/1342>.

1027 Vitousek, P.M., Mooney, H.A., Lubchenco, J., Mellilo, J.M., 1997. Human domination of  
1028 Earth's ecosystems. *Science* 277, 494-499.

1029 Vitvar, T., Aggarwal, P.K., McDonnell, J.J., 2004. A review of isotope applications in  
1030 catchment hydrology. In: P.K. Aggarwal, J. Gat and K. Froehlich (eds.), *Isotopes in the water*  
1031 *cycle: Past, present and future of a developing science*. International Atomic Energy Agency  
1032 Publication, Netherlands, pp 151-169.

1033 Warriar, C.U., Babu, M.P., Manjula, P., Velayudhan, K.T., Shahul Hameed, A., Vasu, K.,  
1034 2001. Isotopic characterization of dual monsoon precipitation-evidence from Kerala, India.  
1035 *Current Science* 98, 1487-1495.

1036 Windhorst, D., Waltz, T., Timbe, E., Frede, H.G., Breuer, L., 2013. Impact of elevation and  
1037 weather patterns on the isotopic composition of precipitation in a tropical montane forest.  
1038 Hydrology and Earth System Sciences 17, 409-419.

1039 Xie, S.P., Xu, H., Saji, N.H., Wang, Y., Liu, W.T., 2006. Role of narrow mountains in large-  
1040 scale organization of Asian monsoon convection. Journal of Climate 19, 3420-3429.

1041 Yadava, M.G., Ramesh, R.N., Pandarinath, K. 2007. A positive 'amount effect' in the  
1042 Sahayadri (Western Ghats) rainfall. Current Science 93, 560-564.

1043

#### 1044 **List of Tables**

1045 **Table 1:** Sampling places during November / December 2013 and October 2014 with location,  
1046 elevation range, distance to the Arabian Sea coast, number of samples (n) and date.

1047

1048 **Table 2:** Physicochemical parameters, elevation, stable water isotope ratio ( $\delta^{18}\text{O}$  and  $\delta^2\text{H}$ ) and  
1049 calculated d-excess for the November/December 2013 and October 2014 samples. Note that GW is for  
1050 groundwater, OW for open well, BW for bore well and sd is for standard deviation.

1051

1052 **Table 3:** Summary of relevant studies on the isotopic elevation effect.

1053

1054 **Table 4:** Multiple Linear Regression results as obtained from the Past program version 3.15. The  
1055 dependent variable was oxygen isotope ratio ( $\delta^{18}\text{O}$ ) and the independent variables were the elevation  
1056 above mean sea level (elevation effect), the distance from the coast (Rayleigh distillation and  
1057 continental effect) and the annual rainfall amount (amount effect).

1058

1059 **List of Figures**

1060 **Fig. 1.a.:** Hydrographic map of Southwest India showing different river basins (written in  
1061 blue) from North to South, of the Krishna river (Tunga, Badra and Vedavati), of the Cauvery  
1062 river (Cauvery itself, Kabini, Moyar and Bhavani) and the main coastal rivers (Swarna,  
1063 Nethravati and Chaliyar). The river basin boundary is represented as black line and the white  
1064 dashed lines correspond to state borders. The higher peaks of the Western Ghats are localised  
1065 in white (Mullayanagiri 1930 m, Kudremukh and Charmadi 1800 m, Tadiandamol 1850 m,  
1066 Chembra 2100 m and Doddabetta 2600 m; above mean sea level). The sampling sites for the  
1067 present study during November 2013 and October 2014 are underlined in black (details in  
1068 Table 1), and the sites previously sampled in dashed line. The different type of sampled water  
1069 is given by the following symbol: rainfall samples as triangle, stream, rivulet and spring as  
1070 circle, groundwater as square, lake and ponds by plus.

1071

1072 **Fig. 1.b.:** Rainfall map of South India showing higher amount along the west coast, parallel to the  
1073 eastern Arabian Sea due to the orographic barrier effect of the Western Ghats for the major southwest  
1074 monsoonal moisture and the drier leeward eastern slopes (Map adapted from [C. Sudhakar Reddy et al.](#)  
1075 [2015](#)). The study area corresponding with Fig. 1.a. is given by the black frame. The location name in  
1076 white corresponds to the available GNIP (Global Network of Isotopes in Precipitation) station except  
1077 for Bakrabail (2013 samples; this study) with values in brackets corresponding to the weighted mean  
1078  $\delta^{18}\text{O}$  values. Note: Belgaum in North Karnataka, elevation 747 m asl, average annual rainfall 1200  
1079 mm, temperature 24.4 °C. Bangalore, in East of Karnataka, elevation 897 m asl, annual rainfall 850  
1080 mm, temperature 24.1°C. Kozhikode (Kunnamangalam) in North Kerala, elevation 20 m asl, annual  
1081 rainfall 3050 mm, temperature 27.9°C. Tirunelveli in Tamil Nadu, elevation 4 m asl, annual rainfall  
1082 750 mm, temperature 29.1°C.

1083

1084 **Fig. 1.c.:** Monthly rainfall (India Meteorological Department, Government of India) during 2013 and  
1085 2014 in coastal districts (include regions stretching between west coast to highlands in the western  
1086 slopes of Western Ghats) like Udupi/Dakshin Kannada (for stations Agumbe and Bakrabail),  
1087 Kasaragod/Kannur (Ezhimala, Thottada), Kozhikode and Thrissur receiving mainly the summer  
1088 monsoon during June – September, and the inland districts (include regions from the Ghats top to  
1089 eastern foothills of the Western Ghats) like Shivamogga (eastern part of Agumbe), Kodagu  
1090 (Madikeri), Wayanad (Gudalur, Sultan Bathery) and Nilgiris (Ooty, Pykara) receiving additional  
1091 winter monsoon during October-December. The sampling period is given by the navy blue rectangles.  
1092 The x-axis represents the months from January to December and the y-axis represents the monthly  
1093 rainfall amount (mm) data. Annual rainfall (mm) of corresponding sampling year is given in legend.

1094

1095 **Fig. 1.d.:** Rainfall variability (rainfall amount data from [www.worldweatheronline.com](http://www.worldweatheronline.com) and  
1096 corresponding station spring/groundwater isotope ratio from our study) along the west coast  
1097 and inland regions adjacent to the Western Ghats, South India.

1098

1099 **Fig. 2.a.:** Relationship between water temperature and oxygen isotope ratio ( $\delta^{18}\text{O}$ ) for the  
1100 November 2013 samples.

1101

1102 **Fig. 2.b.:** Relationship between conductivity and oxygen isotope ratio ( $\delta^{18}\text{O}$ ) for the  
1103 November/December 2013 water samples (Agumbe, Bakrabail, Pykara, Doddabetta, Sultan  
1104 Bathery and Thrissur) and the October 2014 water samples (Ezhimala and Thottada).

1105

1106 **Fig. 3:** Relationship between oxygen isotope ratio ( $\delta^{18}\text{O}$ ) and hydrogen isotope ratio ( $\delta^2\text{H}$ ) for  
1107 the water samples of November/December 2013 and October 2014. The solid blue line



1108 represents the Global Meteoric Water Line ( $\delta^2\text{H} = (8 \times \delta^{18}\text{O}) + 10$ ; Craig, 1961). The  
1109 sampling sites are given from the Northern location i.e. Agumbe ( $13^\circ 30'\text{N}$ ) to the Southern  
1110 location i.e. Thrissur ( $10^\circ 30'\text{N}$ ). All these locations are marked in Figure 1.a. Pykara and  
1111 Ooty samples correspond to the sampling in the Nilgiri range with elevation around 2000 m  
1112 asl.

1113

1114 **Fig. 4:** Relationship between elevation and oxygen isotope ratio ( $\delta^{18}\text{O}$ ) along the mountain  
1115 belt of the Western Ghats. The first regression line in green colour is for the stations below  
1116 2050 m asl and the second line in blue is for the stations beyond 2050 m asl in the Nilgiri  
1117 ranges. The overall slope of 0.31 ‰/100 m for the isotope ratios of water from the west coast  
1118 to the highest elevation (sampled here at 2300 m asl) of the Western Ghats is given in red to  
1119 compare with the reported global isotopic lapse rate (0.28 ‰/100 m; [Poage and Chamberlain,](#)  
1120 [2001](#)). Note the data for Mullyanagiri - Charmadi Ghat ([Lambs et al. 2011](#)) and Kudremukh  
1121 ([Tripti et al. 2016](#)) are from published work.

1122

1123 **Fig. 5:** The variability of oxygen isotope ratio ( $\delta^{18}\text{O}$ ) for nine major sampling locations as a  
1124 function of their distance to the Arabian Sea coast. The grey box corresponds to the mean  
1125 oxygen isotope ratio ( $\delta^{18}\text{O} = -3.1 \pm 0.3\text{‰}$ ; [Tripti et al. 2016](#)) of groundwater in southwest  
1126 coast of India.

1127

1128 **Fig. 6:** Results from NOAA Hysplit simulations for the eight main sampling stations with air  
1129 masses back trajectory up to 5 days.

1130

1131 **Fig. 7:** Plot showing relationship between elevation and oxygen isotope ratio ( $\delta^{18}\text{O}$ ) for  
1132 groundwater in Sri Lanka (July 2012) and Rajasthan (December 2011 and November 2014),  
1133 India (data from [Lambs, under preparation](#)).

1134

1135 **Fig. 8:** The variability of deuterium-excess in the sampled water (lake, pond and bore well  
1136 samples are not included to avoid any effect from evaporation) along the Western Ghats and  
1137 its adjacent slopes during this study. Note that water from the mountains close to the west  
1138 coast of India exhibit higher d-excess range between 3 ‰ and 20 ‰ whereas lower variability  
1139 is observed in inland region corresponding to highest elevations in the Western Ghats  
1140 monitored during this study.

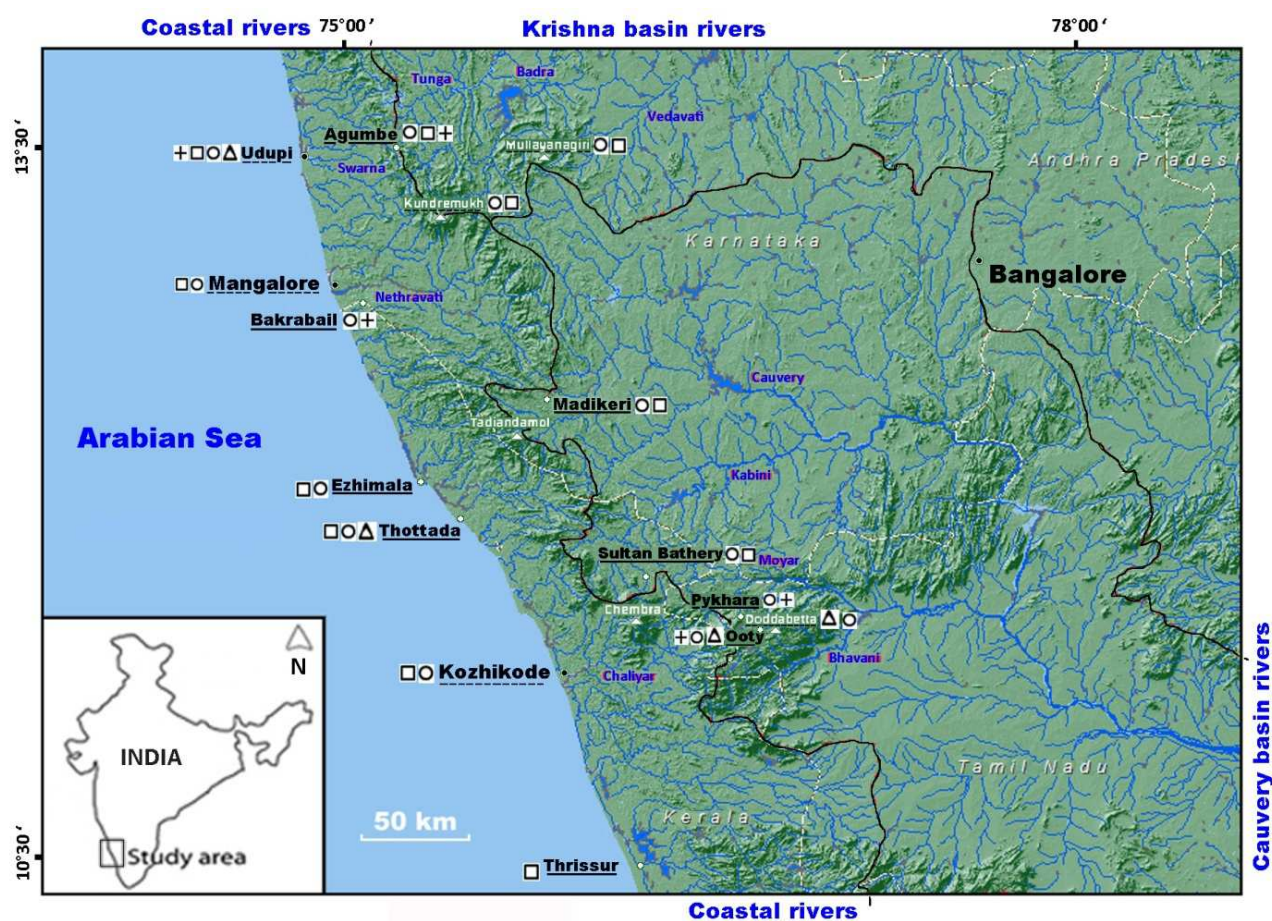


Fig. 1.a.: Hydrographic map of Southwest India showing different river basins (written in blue) from North to South, of the Krishna river (Tunga, Badra and Vedavati), of the Cauvery river (Cauvery itself, Kabini, Moyar and Bhavani) and the main coastal rivers (Swarna, Nethravati and Chaliyar). The river basin boundary is represented as black line and the white dashed lines correspond to state borders. The higher peaks of the Western Ghats are localised in white (Mullayanagiri 1930 m, Kudremukh and Charmadi 1800 m, Tadiandamol 1850 m, Chembra 2100 m and Doddabetta 2600 m; above mean sea level). The sampling sites for the present study during November 2013 and October 2014 are underlined in black (details in Table 1), and the sites previously sampled in dashed line. The different type of sampled water is given by the following symbol: rainfall samples as triangle, stream, rivulet and spring as circle, groundwater as square, lake and ponds by plus.

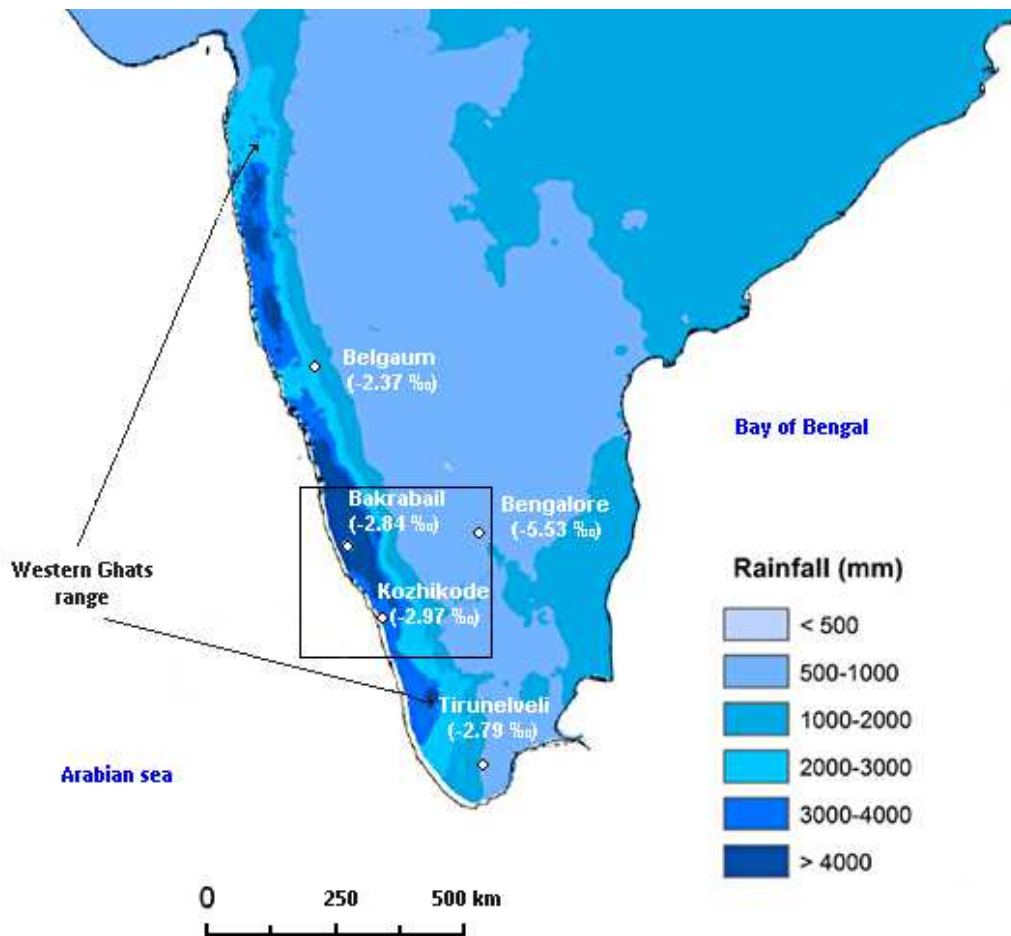
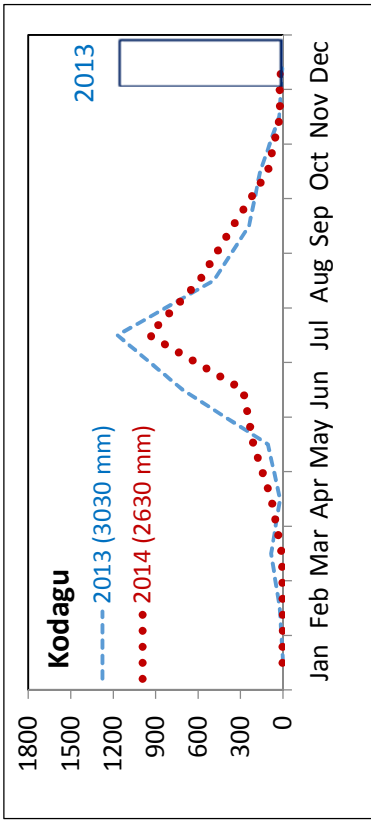
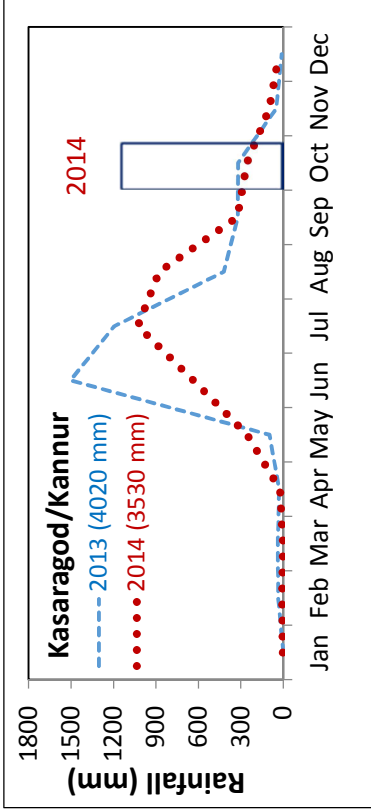
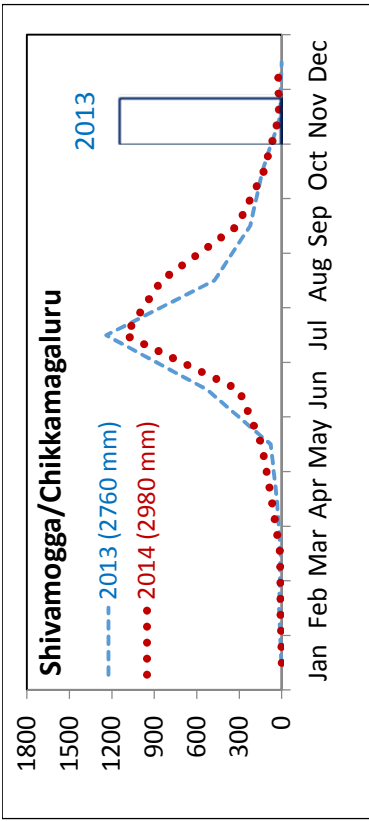
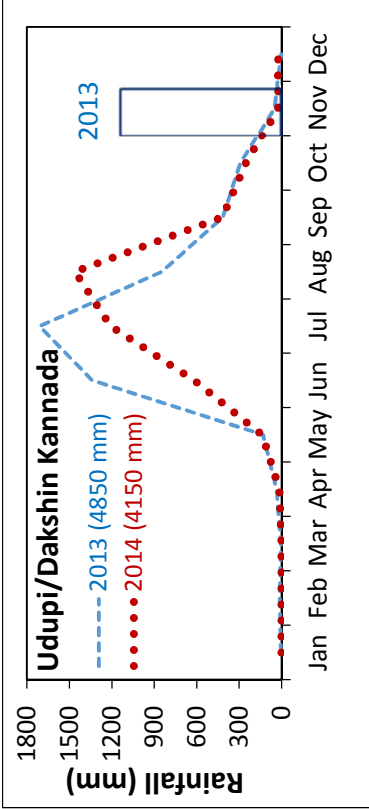


Fig. 1.b.: Rainfall map of South India showing higher amount along the west coast, parallel to the eastern Arabian Sea due to the orographic barrier effect of the Western Ghats for the major southwest monsoonal moisture and the drier leeward eastern slopes (Map adapted from [C. Sudhakar Reddy et al. 2015](#)). The study area corresponding with Fig. 1.a. is given by the black frame. The location name in white corresponds to the available GNIP (Global Network of Isotopes in Precipitation) station except for Bakrabail (2013 samples; this study) with values in brackets corresponding to the weighted mean  $\delta^{18}\text{O}$  values. Note: Belgaum in North Karnataka, elevation 747 m asl, average annual rainfall 1200 mm, temperature 24.4 °C. Bangalore, in East of Karnataka, elevation 897 m asl, annual rainfall 850 mm, temperature 24.1°C. Kozhikode (Kunnamangalam) in North Kerala, elevation 20 m asl, annual rainfall 3050 mm, temperature 27.9°C. Tirunelveli in Tamil Nadu, elevation 4 m asl, annual rainfall 750 mm, temperature 29.1°C.



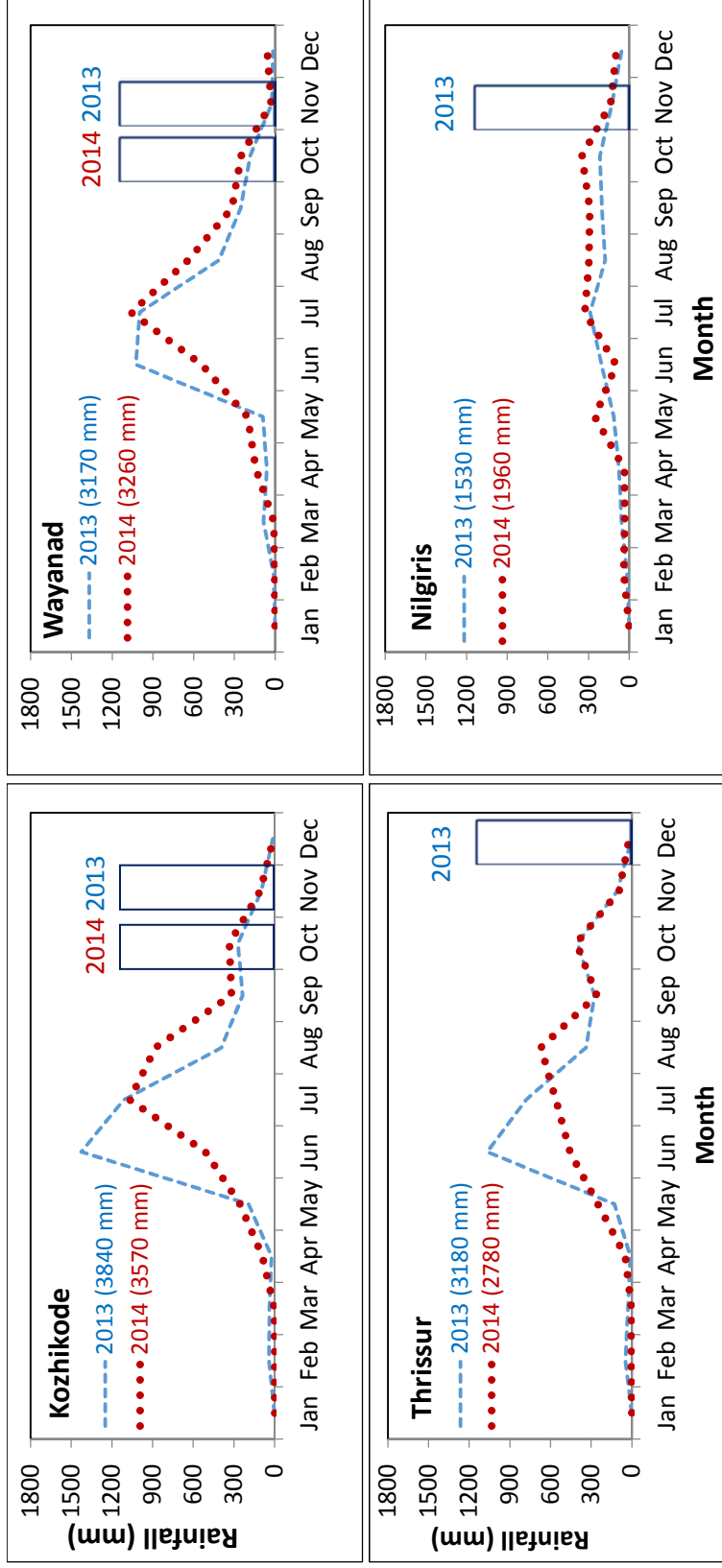


Fig. 1.c.: Monthly rainfall (India Meteorological Department, Government of India) during 2013 and 2014 in coastal districts (include regions stretching between west coast to highlands in the western slopes of Western Ghats) like Udupi/Dakshin Kannada (for stations Agumbe and Bakrabail), Kasaragod/Kannur (Ezhimala, Thottada), Kozhikode and Thrissur receiving mainly the summer monsoon during June – September, and the inland districts (include regions from the Ghats top to eastern foothills of the Western Ghats) like Shivamogga (eastern part of Agumbe), Kodagu (Madikeri), Wayanad (Gudalur, Sultan Bathery) and Nilgiris (Ooty, Pykara) receiving additional winter monsoon during October-December. The sampling period is given by the navy blue rectangles. The x-axis represents the months from January to December and the y-axis represents the monthly rainfall amount (mm) data. Annual rainfall (mm) of corresponding sampling year is given in legend.

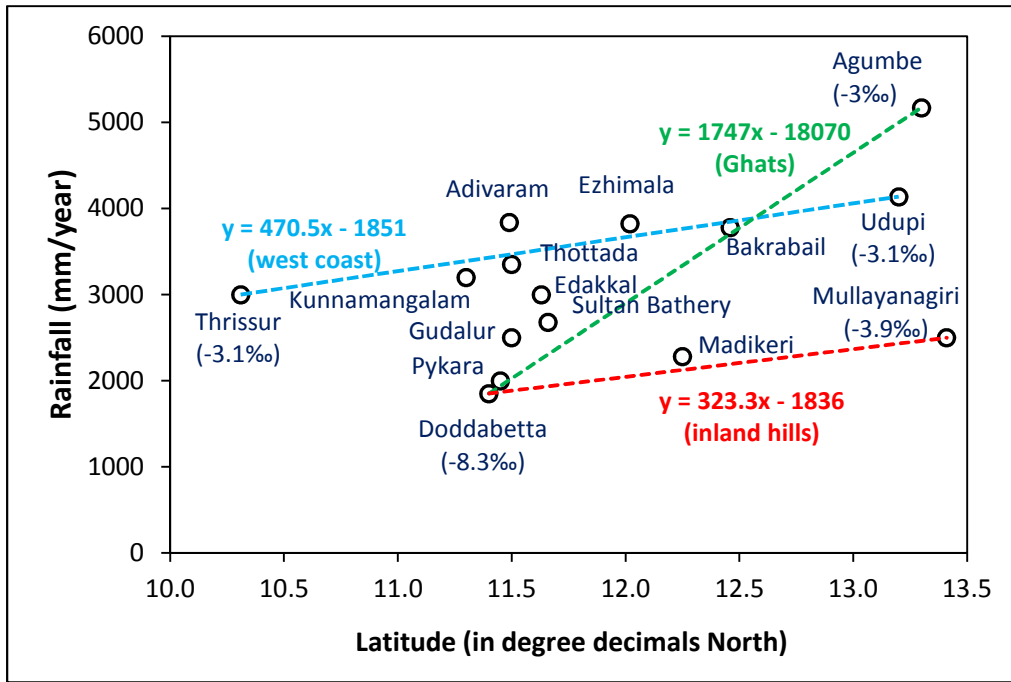


Fig. 1.d.: Rainfall variability (rainfall amount data from [www.worldweatheronline.com](http://www.worldweatheronline.com) and corresponding station spring/groundwater isotope ratio from our study) along the west coast and inland regions adjacent to the Western Ghats, South India.



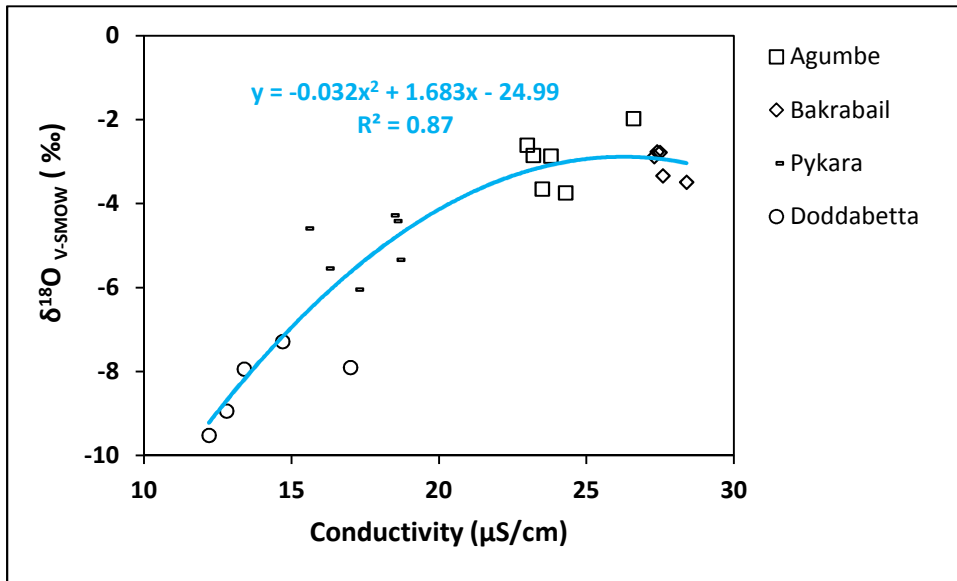


Fig. 2.a.: Relationship between water temperature and oxygen isotope ratio ( $\delta^{18}\text{O}$ ) for the November 2013 samples.

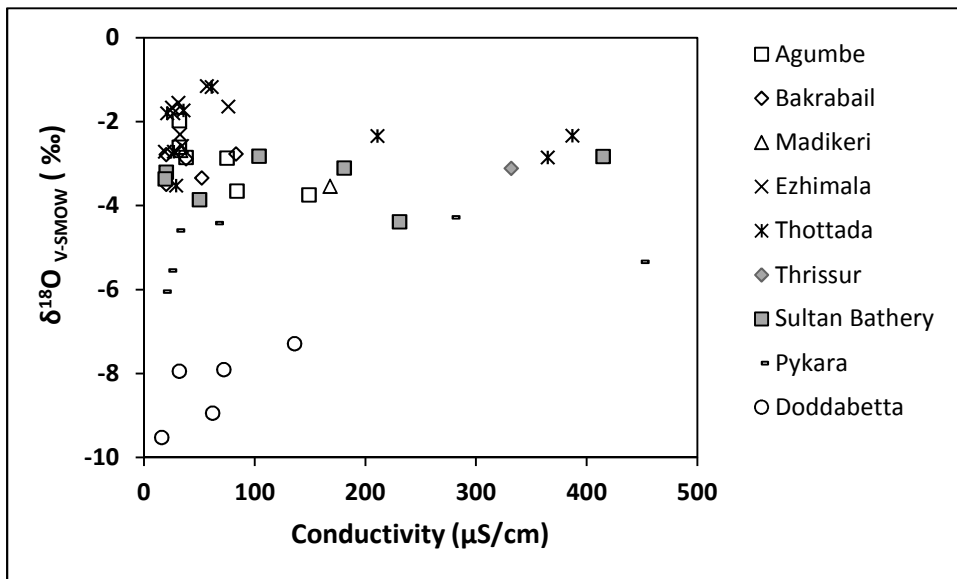


Fig. 2.b.: Relationship between conductivity and oxygen isotope ratio ( $\delta^{18}\text{O}$ ) for the November/December 2013 water samples (Agumbe, Bakrabail, Pykara, Doddabetta, Sultan Bathery and Thrissur) and the October 2014 water samples (Ezhimala and Thottada).



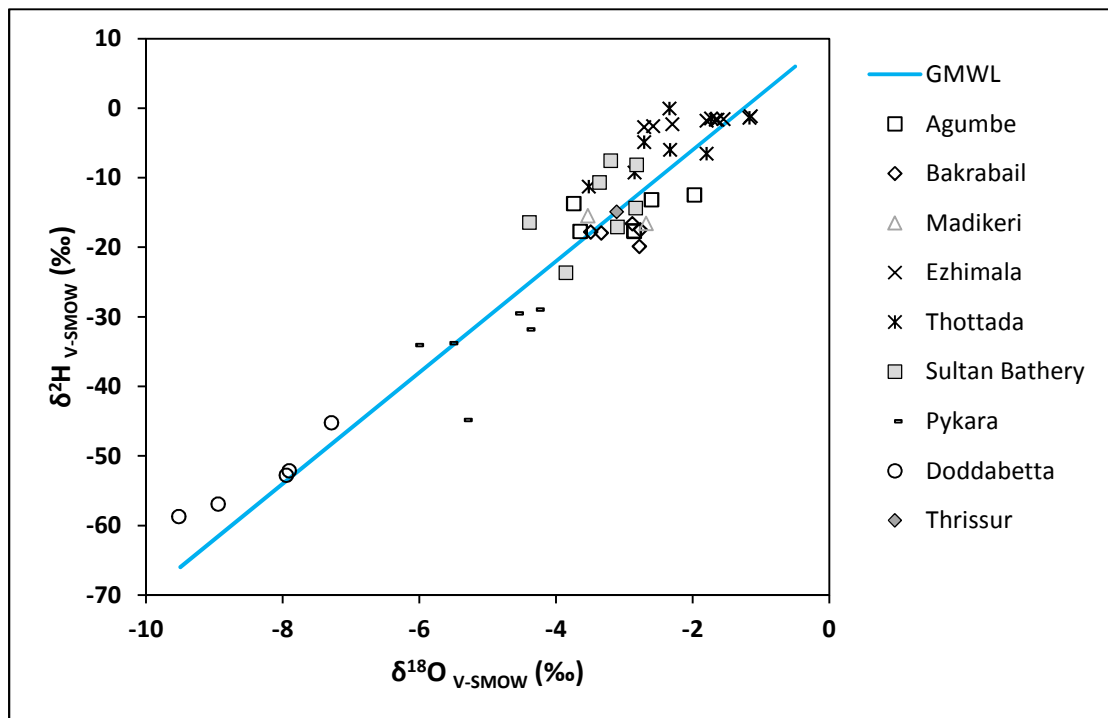


Fig. 3: Relationship between oxygen isotope ratio ( $\delta^{18}\text{O}$ ) and hydrogen isotope ratio ( $\delta^2\text{H}$ ) for the water samples of November/December 2013 and October 2014. The solid blue line represents the Global Meteoric Water Line ( $\delta^2\text{H} = (8 \times \delta^{18}\text{O}) + 10$ ; Craig, 1961). The sampling sites are given from the Northern location i.e. Agumbe ( $13^\circ 30'\text{N}$ ) to the Southern location i.e. Thrissur ( $10^\circ 30'\text{N}$ ). All these locations are marked in Figure 1.a. Pykara and Ooty samples correspond to the sampling in the Nilgiri range with elevation around 2000 m asl.

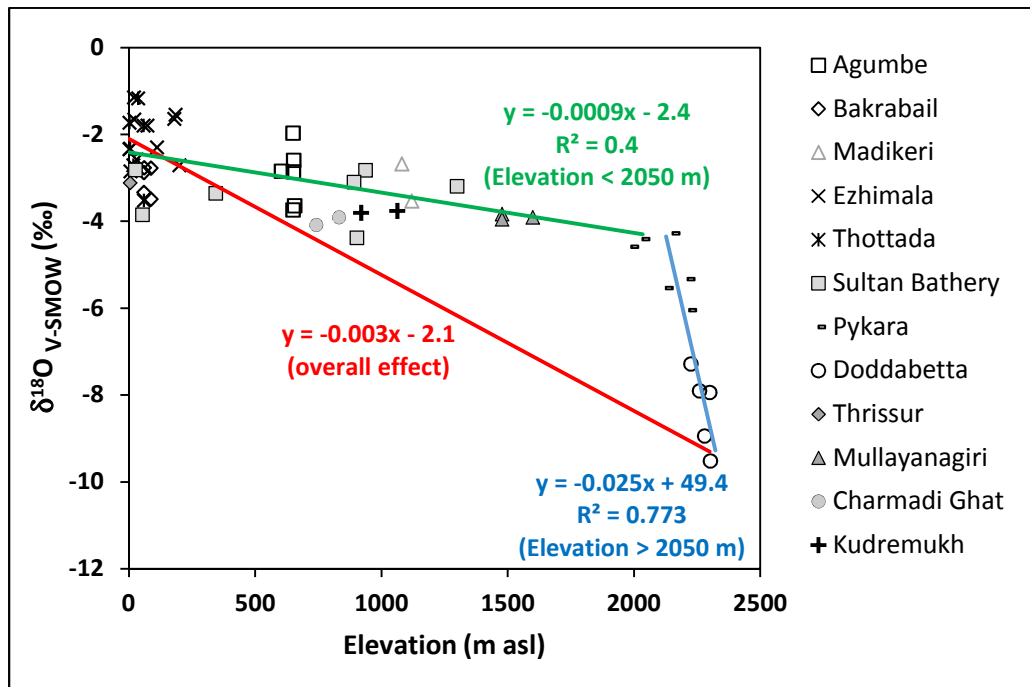


Fig. 4: Relationship between elevation and oxygen isotope ratio ( $\delta^{18}\text{O}$ ) along the mountain belt of the Western Ghats. The first regression line in green colour is for the stations below 2050 m asl and the second line in blue is for the stations beyond 2050 m asl in the Nilgiri ranges. The overall slope of 0.31 ‰/100 m for the isotope ratios of water from the west coast to the highest elevation (sampled here at 2300 m asl) of the Western Ghats is given in red to compare with the reported global isotopic lapse rate (0.28 ‰/100 m; [Poage and Chamberlain, 2001](#)). Note the data for Mullayanagiri - Charmadi Ghat ([Lambs et al. 2011](#)) and Kudremukh ([Tripti et al. 2016](#)) are from published work.

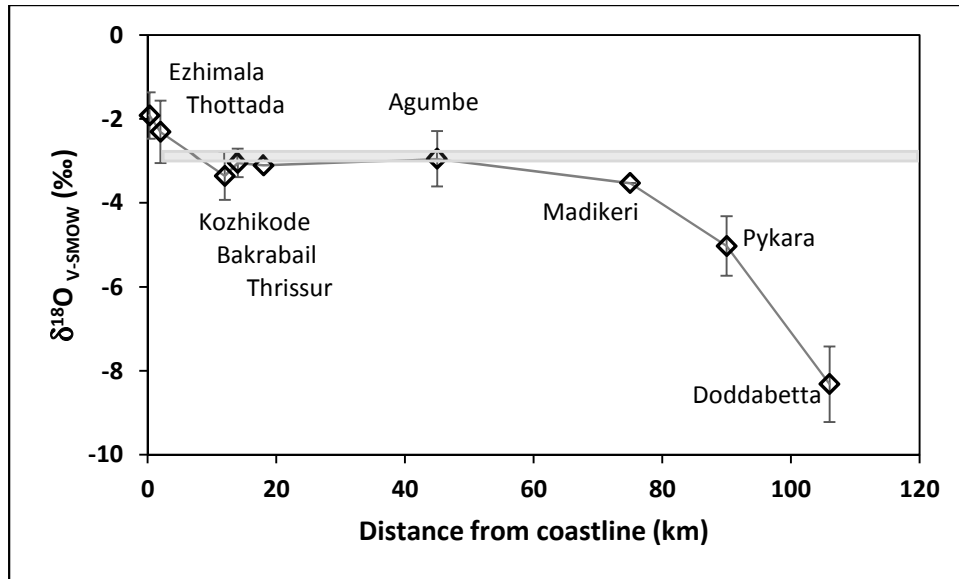
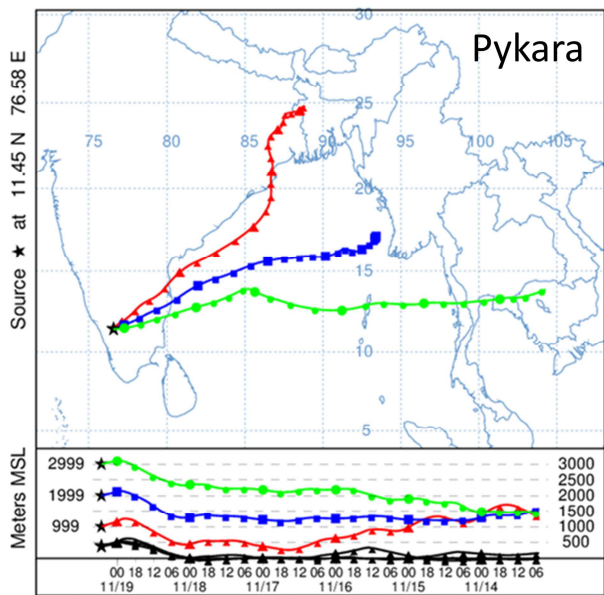
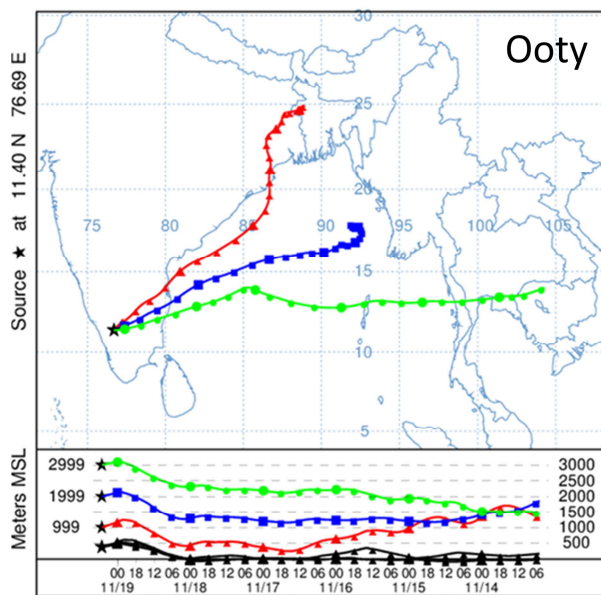
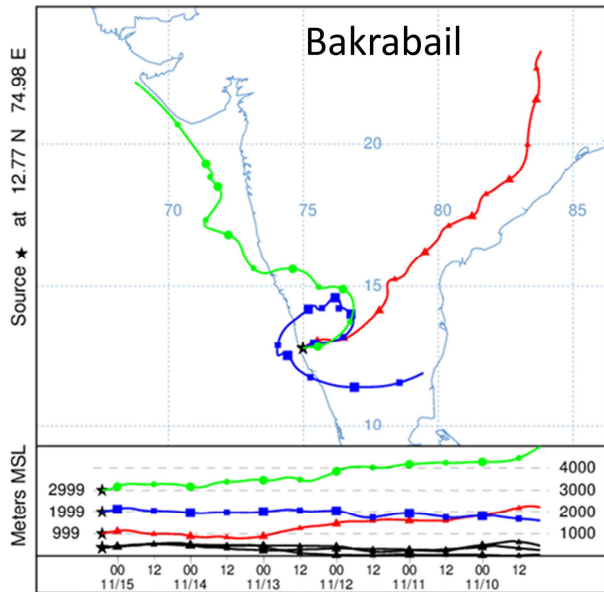
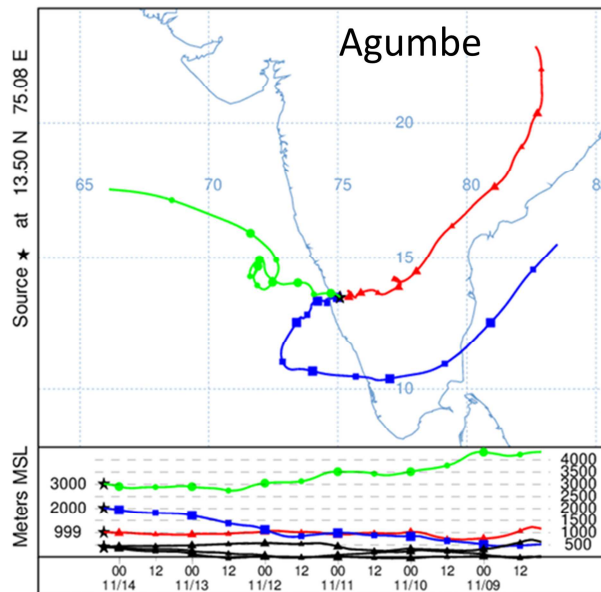


Fig. 5: The variability of oxygen isotope ratio ( $\delta^{18}\text{O}$ ) for nine major sampling locations as a function of their distance to the Arabian Sea coast. The grey box corresponds to the mean oxygen isotope ratio ( $\delta^{18}\text{O} = -3.1 \pm 0.3\text{‰}$ ; [Tripti et al. 2016](#)) of groundwater in southwest coast of India.



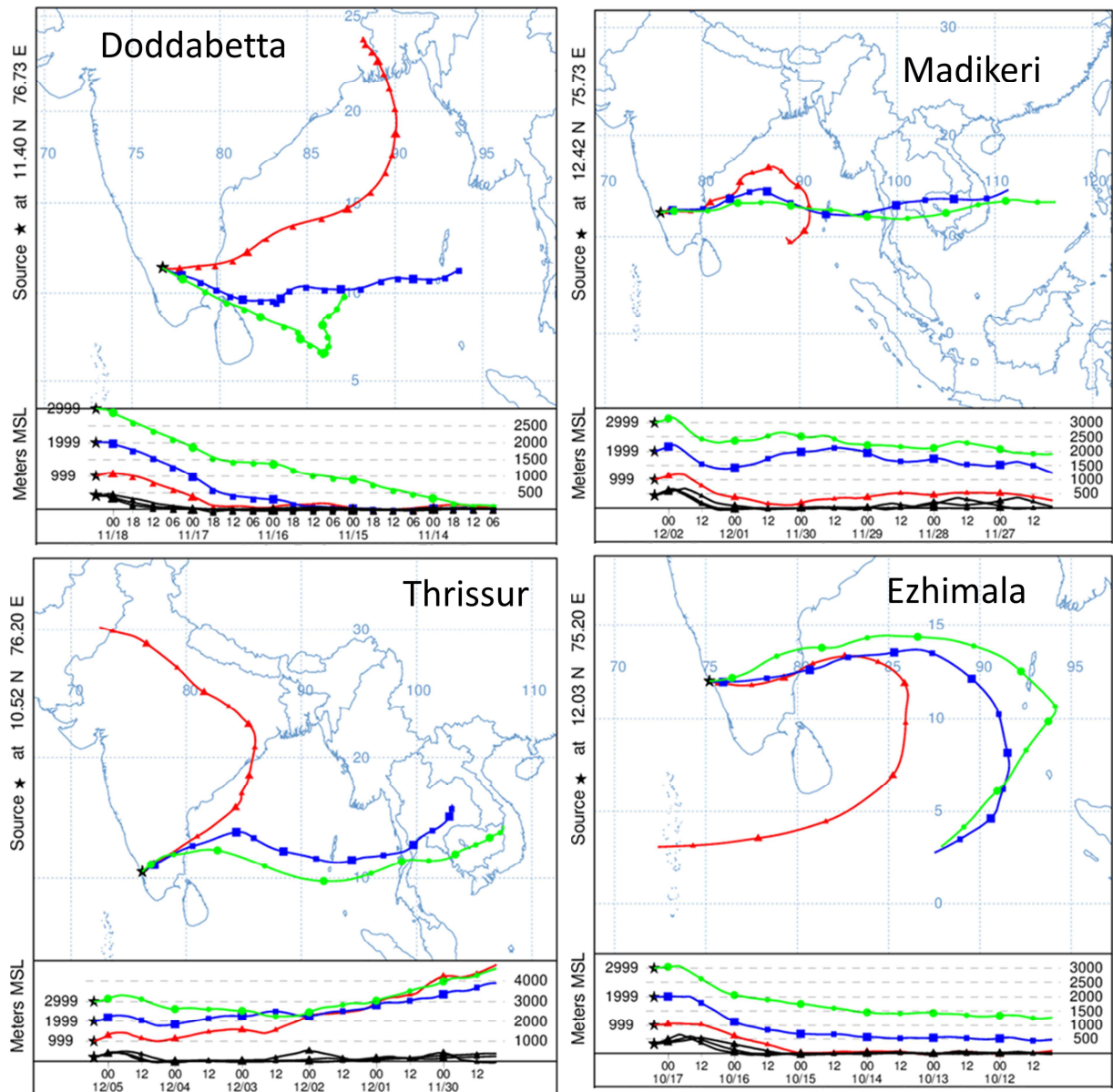


Fig. 6: Results from NOAA Hysplit simulations for the eight main sampling stations with air masses back trajectory up to 5 days.

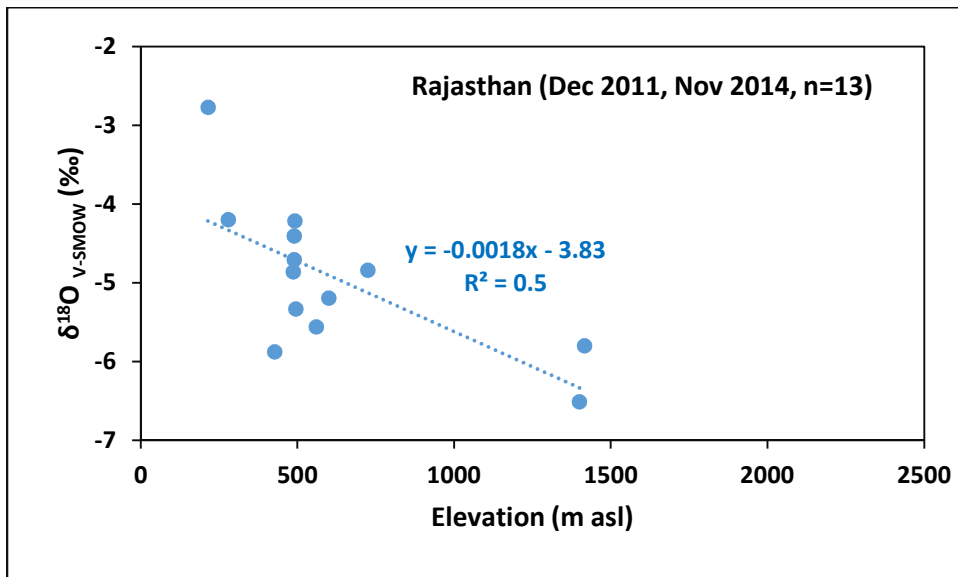
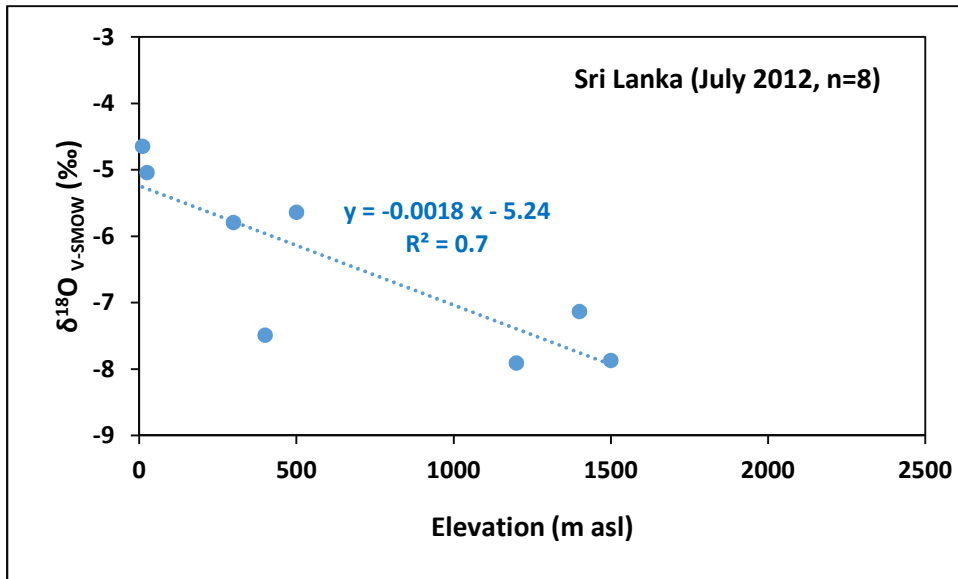


Fig. 7: Plot showing relationship between elevation and oxygen isotope ratio ( $\delta^{18}\text{O}$ ) for groundwater in Sri Lanka (July 2012) and Rajasthan (December 2011 and November 2014), India (data from [Lambs, under preparation](#)).

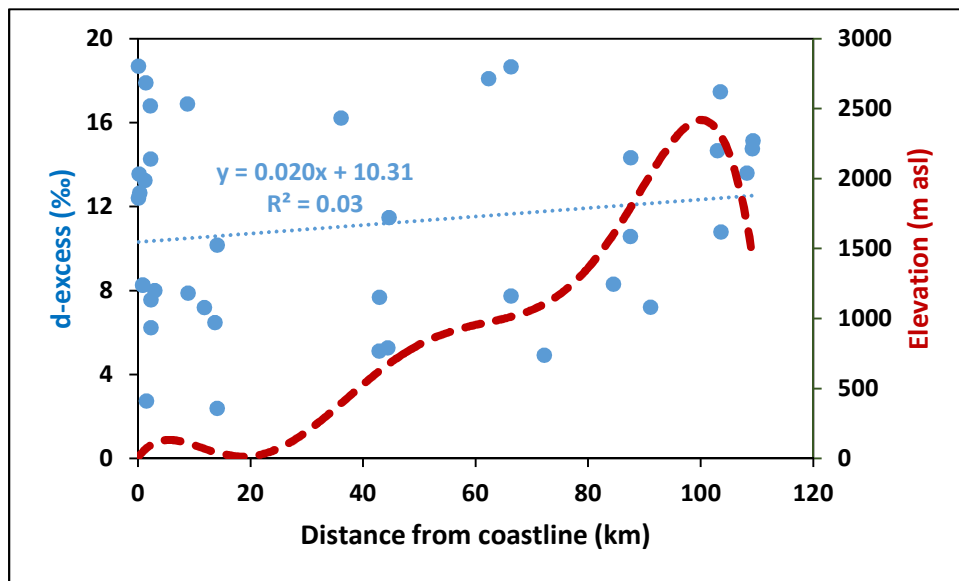


Fig. 8: The variability of deuterium-excess in the sampled water (lake, pond and bore well samples are not included to avoid any effect from evaporation) along the Western Ghats and its adjacent slopes during this study. Note that water from the mountains close to the west coast of India exhibit higher d-excess range between 3 ‰ and 20 ‰ whereas lower variability is observed in inland region corresponding to highest elevations in the Western Ghats monitored during this study.

**Table 1:** Sampling places during November / December 2013 and October 2014 with location, elevation range, distance to the Arabian Sea coast, number of samples (n) and date.

Place	State	Location	Elevation	Sea distance	n	Date
Agumbe	Karnataka	13°30'N, 75°05'E	605-657 m	45 km	6	Nov 2013
Bakrabail	Kerala	12°46'N, 74°59'E	59-100 m	14 km	5	Nov 2013
Madikeri	Karnataka	12°25'N, 75°44'E	1080-1120 m	75 km	2	Dec 2013
Ezhimala	Kerala	12°02'N, 75°12'E	20- 200 m	0.3-2.0 km	8	Oct 2014
Tottada	Kerala	11°50'N, 75°24'E	2-60 m	0.2-18 km	8	Oct 2014
Pykara	Tamil Nadu	11°27'N, 76°35'E	1990-2220 m	90 km	6	Nov 2013
Doddabetta	Tamil Nadu	11°24'N, 76°44'E	2225-2600 m	106 km	7	Nov 2013
Sultan Bathery	Kerala	11°42'N, 76°17'E	27-1300 m	12-85 km	7	Nov 2013, Oct 2014
Thrissur	Kerala	10°31'N, 76°12'E	15 m	18 km	1	Dec 2013



**Table 2:** Physicochemical parameters, elevation, stable water isotope ratio ( $\delta^{18}\text{O}$  and  $\delta^2\text{H}$ ) and calculated d-excess for the November/December 2013 and October 2014 samples. Note that GW is for groundwater, OW for open well, BW for bore well and sd is for standard deviation.

Sl. No.	Location	Type	Date	Conductivity ( $\mu\text{S cm}^{-1}$ )	Temperature ( $^{\circ}\text{C}$ )	Elevation (m asl)	$\delta^{18}\text{O}$ (‰)	$\delta^2\text{H}$ (‰)	d-excess (‰)
1	<u>Agumbe</u>	Pond	14/Nov/2013	32	26.6	650	-1.97	-12.46	3.34
2	Agumbe	GW	14/Nov/2013	32	23	652	-2.60	-13.15	7.68
3	Agumbe	Waterfall	14/Nov/2013	38	23.2	605	-2.85	-17.72	5.12
4	Agumbe	GW-OW1	14/Nov/2013	75	23.8	651	-2.86	-17.63	5.27
5	Agumbe	GW-BW	14/Nov/2013	149	24.3	650	-3.74	-13.72	16.21
6	Agumbe	GW-OW2	14/Nov/2013	84	23.5	657	-3.65	-17.70	11.48
						<b>mean</b>	<b>-2.95</b>	<b>-15.39</b>	<b>8.18</b>
						<b>sd</b>	<b>0.66</b>	<b>2.54</b>	<b>4.84</b>
7	<u>Bakrabail</u>	Pond 1	15/Nov/2013	83	27.4	61	-2.77	-17.47	4.66
8	Bakrabail	Rivulet	15/Nov/2013	38	27.3	59	-2.88	-16.58	6.48
9	Bakrabail	Pond 2	15/Nov/2013	52	27.6	60	-3.34	-17.94	8.78
10	Bakrabail	Spring 2	15/Nov/2013	20	28.4	87	-3.49	-17.78	10.16
11	Bakrabail	Spring 3	15/Nov/2013	20	27.5	88	-2.78	-19.85	2.39
						<b>mean</b>	<b>-3.05</b>	<b>-17.92</b>	<b>6.50</b>
						<b>sd</b>	<b>0.34</b>	<b>1.20</b>	<b>3.12</b>
12	<u>Madikeri</u>	Rivulet	02/Dec/2013	33		1081	-2.68	-16.55	4.92
13	Madikeri	GW BW	02/Dec/2013	168		1120	-3.53	-15.44	12.84
14	<u>Ezhimala</u>	GW OW1	17/Oct/2014	31		185	-1.55	-4.84	7.56
15	Resorthill	Ezhimala	17/Oct/2014	76		180	-1.64	-6.88	6.24
16	Hanuman temple	GW OW2	17/Oct/2014	19		200	-2.71	-7.42	14.26
17	Chittadi	GW OW3	17/Oct/2014	32		112	-2.30	-10.14	8.26
18	Chittadi	Spring	17/Oct/2014	26		73	-1.80	-6.14	8.26
19	Etikulam 1	GW OW1	17/Oct/2014	25		22	-1.66	-0.03	13.25

20	Etikulam 2	GW OW2	17/Oct/2014	34		31	-2.58	-2.74	17.90
21	Etikulam 3	GW OW3	17/Oct/2014	57		20	-1.15	-6.46	2.74
						<b>mean</b>	<b>-1.92</b>	<b>-5.58</b>	<b>9.81</b>
						<b>sd</b>	<b>0.55</b>	<b>3.08</b>	<b>4.93</b>
22	Venagara temple	GW OW1	17/Oct/2014	27		18	-2.71	-4.88	16.80
23	Venagara road	GW OW2	17/Oct/2014	61		37	-1.17	-1.36	8.00
24	Pariyaram	GW OW	17/Oct/2014	29		60	-3.52	-11.27	16.89
25	Pariyaram	Rivulet	17/Oct/2014	21		58	-1.80	-6.52	7.88
26	<u>Tottada</u>	River	18/Oct/2014	365		6	-2.85	-9.25	13.55
27	Tottada	Rivulet	18/Oct/2014	387		5	-2.33	-5.99	12.65
28	Tottada	Rainfall	18/Oct/2014	36		2	-1.73	-1.44	12.40
29	Tottada	GW OW	18/Oct/2014	211		2	-2.34	-0.04	18.68
						<b>mean</b>	<b>-2.31</b>	<b>-5.09</b>	<b>13.36</b>
						<b>sd</b>	<b>0.74</b>	<b>3.99</b>	<b>4.02</b>
30	<u>Pykara</u>	Lake	19/Nov/2013	65	18.5	2034	-4.42	-31.77	3.55
31	Terrace estate	Rivulet	19/Nov/2013	18	17.2	2219	-6.05	-34.04	14.33
32	Bellevue estate	Rivulet	19/Nov/2013	23	16.2	2127	-5.54	-33.78	10.57
33	TR Bazzar	Rivulet	19/Nov/2013	30	15.5	1990	-4.59	-29.48	7.21
34	Sandynulla	Lake	19/Nov/2013	279	18.4	2153	-4.28	-28.94	5.30
35	Ooty lake	Lake	19/Nov/2013	450	18.6	2213	-5.34	-44.79	-2.10
						<b>mean</b>	<b>-5.03</b>	<b>-33.80</b>	<b>6.48</b>
						<b>sd</b>	<b>0.71</b>	<b>5.78</b>	<b>5.70</b>
36	Ooty	Rainfall 1	17/Nov/2013	30		2225	-17.91	-125.68	17.60
37	Doddabetta	Rainfall 2	17/Nov/2013	13	13.8	2632	-16.03	-107.41	20.82
38	Ooty	GW	18/Nov/2013	136	14.7	2225	-7.29	-45.21	13.09
39	<u>Doddabetta</u>	GW tank	18/Nov/2013	32	13.4	2300	-7.95	-52.77	10.80
40	Doddabetta	Spring Tank-	18/Nov/2013	16	12.2	2302	-9.52	-58.69	17.47
41	Doddabetta	rivulet	18/Nov/2013	62	12.8	2280	-8.94	-56.89	14.66
42	Kodapamund	GW BW	18/Nov/2013	72	17.2	2260	-7.90	-52.14	11.08
						<b>mean</b>	<b>-8.32</b>	<b>-53.14</b>	<b>13.42</b>
						<b>sd</b>	<b>0.90</b>	<b>5.22</b>	<b>2.76</b>
43	Gudalur	GW	20/Nov/2013	415		938	-2.83	-14.34	8.31

---

44	<u>Sultan Bathery</u>	GW	20/Nov/2013	231	904	-4.39	-16.43	18.66
45	Sultan Bathery	GW OW	23/Oct/2014	181	892	-3.10	-17.06	7.74
46	Edakkal	Spring	23/Oct/2014	20	1300	-3.20	-7.51	18.09
47	Adivaram	Rivulet	23/Oct/2014	19	345	-3.36	-10.65	16.23
48	Kunnamangalam	GW	21/Nov/2013	50	55	-3.85	-23.65	7.19
49	Karanthur	GW BW	23/Oct/2014	104	27	-2.82	-8.13	14.43
					<b>mean</b>	<b>-3.36</b>	<b>-13.97</b>	<b>12.95</b>
					<i>sd</i>	<b>0.57</b>	<b>5.72</b>	<b>5.06</b>
50	<u>Thrissur</u>	GW BW	05/Dec/2013	332	5	-3.11	-14.91	9.99

---

**Table 3:** Summary of relevant studies on the isotopic elevation effect.

Sl. No.	Study	Aim of the study	Location	Key findings
1	Dansgaard (1964)	Determining factors influencing fractionation of water isotopes.	Worldwide	The heavy isotope composition in freshwater decreases with latitude and elevation.
2	Ambach et al. (1968)	To measure isotopic elevation, change of rainfall in mountains.	Alps	Isotopic elevation effect of -0.2 ‰/100 m.
3	Siegenthaler and Oeschger (1980)	Variation of $\delta^{18}\text{O}$ with temperature and elevation.	Alps	Isotopic elevation effect of $-0.45 \pm 0.1$ ‰/100 m.
4	Yurtsever and Gat (1981)	Elevation effect on water isotope ratios.	GNIP data, worldwide	Isotopic elevation effect of -0.15 to -0.5 ‰/100 m.
5	Gonfiantini et al. (2001)	Elevation effect on the isotopic composition of tropical rains.	Cameroon and Bolivia	Cameroon -0.16 ‰ and Bolivia -0.24 ‰/100 m.
6	Poage and Chamberlain (2001)	Review of 68 studies on isotopic elevation effect.	World wide	Global mean: -0.28 ‰/100 m; Less effect in tropical area: -0.12 to -0.20 ‰/100 m; Higher effect in extreme conditions: -0.62 to -1.83 ‰/100m.
7	Deshpande et al. (2003)	Study of groundwater isotopic composition.	South India	Possible elevation effect of -0.4 ‰/100 m.
8	Scholl et al. (2009)	Orographic rainfall and amount effects.	Puerto Rico	Isotopic elevation effect of -0.12 ‰/100 m.
9	Windhorst et al. (2013)	Effect of elevation and weather condition on event based precipitation.	Ecuador	Isotopic elevation effect of -0.22 ‰/100 m for elevation range of 1800 – 2800 m asl.
10	Resmi et al. (2016)	Precipitation in Pamba river basin.	Kerala, India	Isotopic elevation effect of -0.1 ‰/100 m.
11	Edirisinghe et al. (2017)	Precipitation over northeast and central Sri Lanka.	Sri Lanka	Isotopic elevation effect of -0.6 ‰/100 m.
12	This study	Orographic upliftment effect on isotope ratios of groundwater and spring water.	South India	Isotopic elevation effect of: -0.09 ‰/100m, below 2050 m asl; -1.5 to -2.5 ‰/100m, beyond 2000 m asl; Mean value of -0.30 ‰/100m (0 - 2500 m asl).

**Table 4:** Multiple Linear Regression results as obtained from the Past program version 3.15. The dependent variable was oxygen isotope ratio ( $\delta^{18}\text{O}$ ) and the independent variables were the elevation above mean sea level (elevation effect), the distance from the coast (Rayleigh distillation and continental effect) and the annual rainfall amount (amount effect).

Number of point	Variable	F	R <sup>2</sup>	p	Significance
51 (all)	<u>isotope values</u>	35.91	0.70	<0.0001	yes
	elevation		0.68	0.0002	yes
	continental		0.56	0.18	no
	amount		0.40	0.39	no
42 (below 2050 m)	<u>isotope values</u>	10.61	0.46	<0.0001	yes
	elevation		0.41	0.96	no
	continental		0.45	0.11	no
	amount		0.12	0.62	no
9 (over 2050 m)	<u>isotopes values</u>	17.33	0.96	0.004	yes
	elevation		0.77	0.08	yes
	continental		0.36	0.21	no
	amount		0.81	0.04	yes